Design of a Hoverwing Aircraft

A project present to
The Faculty of the Department of Aerospace Engineering
San Jose State University
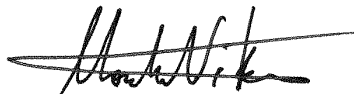
in partial fulfillment of the requirements for the degree
Master of Science in Aerospace Engineering

By

Nita B Shah

May 2011

approved by

Dr. Nikos Mourtos
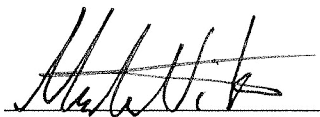Faculty Advisor

San José State
UNIVERSITY

The Undersigned Faculty Committee Approves

Design of a Hoverwing Aircraft

By

Nita B Shah

APPROVED FOR THE DEPARTMENT OF MECHANICAL AND AEROSPACE

ENGINEERING

Dr. Nikos Mourtos, Committee Chair   5/18/11
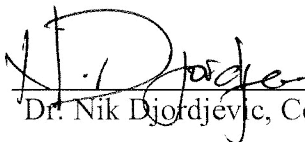   Date

Dr. Periklis Papadopoulos, Committee Member   5/16/2011
                                                                 Date

Dr. Nik Djordjevic, Committee Member   5/17/2011
                                                                 Date

iii

Abstract

Wing-in-Ground effect aircraft is one that manages level flight near the surface of the Earth, making use of the aerodynamic interaction between the wings and the surface known as take advantage ground effect. Ground effect is a phenomenon that relates to the airflow around a wing when it flies in close proximity to a surface, wherein the presence of the surface distorts the downwash from the wing and inhibits the formation of vortices. This effect dramatically increases the lift and reduces the drag compared to that attainable by a wing in conventional flight. The WIG crafts can transport heavy payloads at relatively high speeds, compared to ships. Since the 1960''s, There have been many experiments on Wing in Ground Effect crafts and the Ekranoplan. While some believe that it will bring a new era of high speed marine transportation, others believe it holds less promise than the hovercraft. This paper presents a Wing-In-Ground effect craft design as an alternative to the current ships, a means of faster and safer transportation over water. An initial design is presented for a rigid airship that has the capacity for 16,000 lbs of payload and 2 crew members with 497 miles of range.

Acknowledgement

I would like to thank all people who have helped and inspired me during my graduate study.

I especially want to thank my advisor, Dr. Nikos Mourtos, for his guidance during my project and study at San Jose State University. His perpetual energy and enthusiasm in aerospace field had motivated all his advisees, including me. In addition, he was always accessible and willing to help his students with their research.

I was delighted to interact with Prof. Nik Djordjevic and Dr. Periklis Papadopoulos by attending their classes and having them as my co-advisors. They deserve special thanks as my thesis committee members and advisors.

My deepest gratitude goes to my family for their unflagging love and support throughout my life; this dissertation is simply impossible without them. I am indebted to my parents, Bhadresh and Meena Shah, for their care and love. As typical parents in an Indian family, my parents worked industriously to support the family and spare no effort to provide the best possible environment for me to grow up and attend school. They had never complained in spite of all the hardships in their life. They uprooted their life in India and moved to United States, so that my sister and I could have a good education and a comfortable life. I cannot ask for more from my mother, Meena Shah, as she is simply perfect. I have no suitable word that can fully describe her everlasting love to me. I remember many sleepless nights with her accompanying me when I was ill. I remember

her constant support when I encountered difficulties and I remember, most of all, her delicious dishes. I feel proud of my sister, Neha Shah, for her talents. She had been a role model for me to follow unconsciously when I was a teenager and has always been one of my best counselors. I am extremely lucky to have my fiancé, Michael Trettin, who has supported me through some of the hardest years and I would like to take this opportunity to thank him. He has taken many trips to San Jose State University to submit the reports for my classes when I was not able to go. Without his support and love, I would not have been able to come this far.

Last but not least, thanks be to God for my life through all tests in the past four years. You have made my life more bountiful. May your name be exalted, honored, and glorified.

Table of Contents

viii

Listof Tables

Listof Figures

Nomenclature

Definition	Symbol
g	Acceleration of gravity
$\mathring{a}\ C_f$	Additional friction coefficient for roughness of the plate
A.C.	Aerodynamic Center
$C_{L\underset{.}{I}}$	Airplane lift curve slope
ê	Air Density
3_g	Airplane mass ratio
D_a	Air profile resistance
A	Aspect ratio
W_{struct}	Airplane structural weight
W_A	Airframe weight
C_p	Center of pressure
C_f	Coefficient of water friction on a smooth plate
C_w	Coefficient of wave-making
W_{crew}	Crew Weight
C_{D_o}	Clean zero lift drag coefficient
V_C	Cruising speed
C.G.	Centre of gravity
Vcr	Cruise speed
B_c	Cushion width of air channel
P_c	Cushion pressure in the air channel

C_D	Drag Coefficient
D	Drag
D_{hf}	Drag caused by water friction of hull and sidewalls
D_{swf}	Drag caused by water friction of sidewalls
$Ł$	Dihedral angle
$d\dot{I}/dĮ$	Down wash gradient
U_{de}	Derived gust velocity
V_c	Design cruising speed
W_{empty}	Empty Weight
k	Empirical constant factor
d_f	Equivalent fuselage diameter
C_f	Equivalent skin friction drag
f	Equivalent parasite area
GW	Flight design gross weight
V'	Free stream velocity
$F.S.$	Fuselage station
S_{wetfus}	Fuselage wetted area
D_f	Fuselage diameter
l_f	Fuselage length
W_{fuel}	Fuel Weight
W_{feq}	Fixed equipment weight

D_{fl}	Fouling drag
S	Gross area
S_h	Horizontal size of the empennage
V_h	Horizontal volume coefficient
C_{r_h}	Horizontal tail root chord length
C_{t_h}	Horizontal tail tip chord length
$b_{h/2}$	Horizontal tail span
C_h	Horizontal tail mean geometric chord
$C_{L_{\downarrow h}}$	Horizontal tail lift curve slope
S_{wet_h}	Horizontal tail wetted area
i	Incidence angle
$\hat{U}_w$	Kinetic viscosity coefficient
L/D	Lift-to-drag ratio
n_{lim}	Limit maneuvering load factor
M_{ff}	Mission fuel fraction
M_{tfo}	Mission trapped fuel and oil
W_{MZF}	Mission zero fuel weight
$C_{L_{maxTO}}$	Maximum take-off lift coefficient
$C_{L_{maxL}}$	Maximum landing lift coefficient

V_A	Maneuvering speed
$C_{N_{max}}$	Maximum normal coefficient
$C_{L_{max}}$	Maximum lift coefficient
$C_{N_{maxneg}}$	Maximum negative lift coefficient
$\bar{c}$	Mean geometric chord
V_{max}	Maximum design speed
n_p	Number of blades
N_{crew}	Number of crew
N_e	Number of engines per airplane
N_p	Number of propellers per airplane
N_{pax}	Number of passengers
n_{ac}	Number of air channels on the craft
e	Oswald''s efficiency factor
$W_{payload}$	Payload Weight
W_{pwr}	Power plant weight
P_{bl}	Power loading per blade
W/P	Power loading
$\bar{x}_{ac_A}$	Position of A.C. on wing mean geometric chord
$\bar{x}_{ach}$	Position of horizontal tail on wing mean geometric chord
S_{wet}	Plan form wetted area

M_{res}	Reserve fuel fraction
C_r	Root chord
$Ş_h$	Ratio of horizontal to wing dynamic pressure
S_a	Reference area for calculating the air profile drag and lift
V_{stall}	Stalling velocity
C_{fe}	Skin friction coefficient
b	Span
$K_{\dot{a}}$	Sweep correction factor
C_{l_f}	Section lift curve slope with flaps down
C_{l}	Section lift curve slope
$\acute{a}_{c/4}$	Sweep angle
$\square_{c_2}$	Semi chord sweep angle
$\square$	Side slip angle
V_S	Stall speed
V	Speed
SES	Surface Effect Ship
T/W	Thrust-to-Weight ratio
W_o	Takeoff gross weight
T	Thrust

□	Taper ratio
C_t	Tip chord
t/c	Thickness ratio
W_{TO}	Take off weight
D_t	Propeller diameter
t/c	Thickness ratio
T_{TO}	Tooling total take off thrust
S_v	Vertical size of the empennage
V_v	Vertical volume coefficient
C_{rv}	Vertical tail root chord length
C_{tv}	Vertical tail tip chord length
b_v	Vertical tail span
C_v	Vertical tail mean geometric chord length
$C_{L_{l_v}}$	Vertical lift curve slope
S_{wet_v}	Vertical tail wetted area
W/S	Wing Loading
S	Wing area
C	Wing mean geometric chord
b	Wing span

$C_{L_{I_W}}$ Wing lift curve slope

$C_{L_{I_{wf}}}$ Wing fuselage (wing body) lift curve slope

K_{wf} Wing fuselage interference factor

W_{eng} Weight per engine

W Weight

L Wetted length of hull or side buoys

S_{hf} Wetted surface areas of the hull

S_{swf} Wetted surface areas of the sidewall

Chapter 1. Motivation – Mission Profile

1.1. Motivation

In recent years, the need for fast transport between and around many coastal cities has become important for both work and recreational travel. The development of tourism has increased the need for ferry operators, which in turn led to the discovery of new vehicle types with higher speed and greater transport efficiency. The main reason to build a wing-in-ground effect craft (WIG) is payload capacity and cost. WIG crafts have the potential for payload capacities closer to fast marine crafts and the cost of construction is much lower than aircrafts [1]. The Hoverwing can also be used in paramilitary applications that include littoral operations, drug-running interdiction, anti-piracy, border patrol, search and rescue, etc. In addition, the WIG crafts may be difficult to detect by mines or sonar, making them suitable for crossing minefields and mine clearance.

 WIG crafts allow for high speed marine transportation at 100 knots in comfort, without water contact, slamming shock, stress, wake, wash or seasickness. These crafts are extremely fuel efficient. The ability of WIG crafts to handle sea state opens the potential usage to coastal, inter island, and major rivers. Hundreds of millions of people living and working in these locations would benefit from WIG crafts. WIG crafts have many benefits:

- x Faster travel allows for more trips, customers, and thereby more revenue

- x Brings new destinations closer

- x New routes becomes possible

There are benefits of zero water contact such as no sea motion or sea sickness, low fatigue for passengers, no wash, shallow water operations. Due to these benefits, WIG crafts would be ideal for a civilian market [1].

This project is to design a WIG craft, called Hoverwing. The idea of this craft is based on current WIG projects taking place in Germany. Mr. Hanno Fischer has successfully developed and tested a 2-seater WIG craft called Hoverwing 2VT. His future designs, according to his website, include developing WIG crafts for 15, 20, and 80 passenger and so on Hoverwing crafts. This project is to design a Hoverwing that carries 8-tons of payload. The base parameters, such as takeoff weight, span and maximum speed, were taken from Mr. Fischer''s Hoverwing 80 project to initiate this project [2].

Hoverwing is a second generation WIG craft, which means that it uses static air cushion for take-off, similar to SES and hovercrafts. A hovercraft or SES-like static air cushion is sealed all around and air is injected into the cavity under the wing; in Hoverwing craft''s case, the air is sealed under the fuselage. The amount of air and the pressure of the air are much lower than with Power Augmentation (PAR). PAR or air injection is the principle of a jet or propeller in front of the wing that blows under the wing at take-off. The cavity under the wing is bounded by endplates and flaps, so that the air is trapped under the wing. This way the full weight of the WIG boat can even be lifted at zero forward speed. The Hoverwing uses air from the propeller that is captured by a door in the engine pylon to power up the cushion. Some

other designs propose a very low power auxiliary fan for this purpose.

This report includes the detail work of calculating important

parameters

such as empty weight, fuel weight, drag coefficient along with developing the sizes for wings and its control surfaces, vertical and horizontal tails, and fuselage.

1.2. Mission specification

Table 1. Mission Specification

Range	497 miles
Takeoff Wave Height	5 ft
Cruising Wave Height	7 ft
Cruise altitude	15 ft
Number of Crew members	2
Payload Capacity	16,820 lbs
Number of Engines	1
Engine Type	Turboprop
Takeoff Field Length	3280 ft
Landing Fiend Length	3280 ft
Cruise Speed	125 knots

1.2.1. Mission profile

The first step in designing any craft is to develop mission requirements and identify critical requirements. For Hoverwing, the mission requirements and critical requirements are shown in Appendices A and B. A Hoverwing starts in displacement mode at lower speed to accelerate from stand still to its normal service speed over water. After displacement mode, it transits from planning mode to flying mode. During transition, the

craft operates as a hydroplane. A hydroplane uses the water it''s on for lift, as well as propulsion and steering. When traveling at high speed water is forced downwards by the bottom of the boat's hull. The water therefore exerts an equal and opposite force upwards, lifting the vast majority of the hull out of the water.
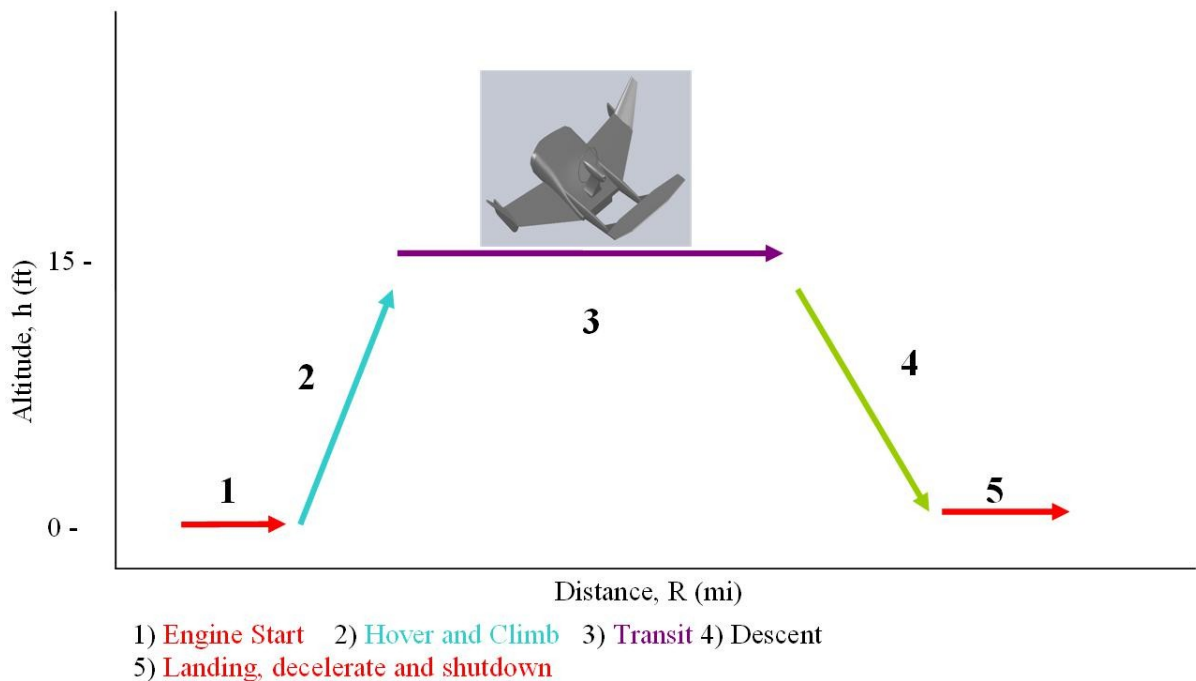
Figure 1. Mission profile of hoverwing

1.2.2. Market analysis

The technology of the WIG effect craft is fairly new. A WIG craft is a high-speed ""dynamic hovercraft"" surface/marine vehicle. Most WIG crafts have been developed from analytical theory, model testing and building prototypes. WIG craft theory and technology covers wide range of possible craft configurations. WIG craft size and speed ranges from single passenger prototypes operating at 50 km/h to large military craft at 500 km/h. The largest WIG craft build to-date is KM. With a length of 348 ft and wing

span of 131 ft, KM is able to transport 550 tons of cargo. Due to its massive size, the KM is also known as Caspian Sea Monster. The next vehicle in KM family was ""Orlyonok"". It was introduced in 1973 with 120-ton takeoff weight and AR of the main wing 3 [3]. Another type of Russian WIG craft is known as DACS, Dynamic Air Cushion Ships. The basic element of DACS is a wing of small aspect ratio bounded by floats and rear flaps to form a chamber. The dynamic air cushion chamber under a wing is formed by blowing of the air with propellers mounted in front of the vehicle. For DACS, blowing air is a permanent feature present during cruising and takeoff-touchdown modes. Though the efficiency of DACS is similar to that of hydrofoil ships, the speed of DACS far exceeds that of hydrofoil ships. The first practical vehicle of DACS type was the Volga-2, which was capable of transporting 2.7 ton weight with a cruising speed of 100 to 140 km/h. The development and design of WIG craft started in 1967 in China. In 30 years, China has designed and tested 9 small manned WIG crafts. The XTW series were developed in 1996 by China Ship Scientific Research Center (CSSRC). Later on, 20-seat passenger WIG effect ship was first tested in 1999. The 6-seater SDJ 1 was developed using catamaran configuration. In 1980s, another Chinese organization, MARIC, started developing Amphibious WIG crafts. After successfully testing 30 kg radio controlled model, MARIC developed and tested WIG-750 with a maximum TOW of 745 kg. In 1995, the China State Shipbuilding Corporation completed AWIG-751 named, ""Swan-I"". It has maximum TOW of 8.1tons and cruising speed of 130 km/h. Later on, AWIG-750

was developed; it had several new features including: increased span of the main wing, composite wing, combined use of guide vanes and flaps to enhance longitudinal stability.

Tests confirmed overall compliance with the design requirements, but showed some disadvantages, such as too long shaft drives of the bow propellers, lower payload and lower ground clearance than expected. AWIG-751G, also known as ""Swan-II"", had increased dimensions and an improved composite wing [3].

In 1963, Lippisch, a German aerodynamicist, introduced new WIG effect vehicle based on the reverse delta wing planform. He built first X-112 ""Airfoil Boat"". This and the following Lippisch craft had a moderate aspect ratio of 3 and inverse dihedral of the main wing enabling them to elevate the hull with respect to the water surface. The reported lift-to-drag ratios were in order of 25. In Germany, Hanno Fischer developed his own company ""Fischer Flugmechanik"" and extended Lippisch design concept to develop and build a 2-seat vehicle, known as Airfish FF1/FF2. The Airfish was designed to fly only in ground effect unlike X-112 and X-114. The Airfish was reported to have speed of 100 km/h at just half the engine''s power during tests in 1988. Later on, the company developed 4-seater Airfish-3. Although the craft was designed to use in ground effect, it could perform temporary dynamic jumps climbing to a height of 4.5 m. A design series of Airfish led to Flightship 8. The FS-8 can transport 8 people, including two crew members. It has cruising speed of 160 km/h and a range of 365 km. The originators of FS-8 design Fischer Flugmechanik and AFD Aerofoil Development GmbH have recently announced a proposal to produce a new craft called hoverwing-20. The hoverwing technology employs a simple system of retractable flexible skirts to

retain an air cushion between the catamaran of the main hull

configuration. This static air cushion is used only

during takeoff, thus enabling the vehicle to accelerate with minimal power before making a seamless transition to ground effect mode.

The motivation for designing the hoverwing airplane is to find a cheaper and faster means of travel in coastal areas. The hoverwing airplanes are aimed at markets in coastal, interisland, estuary and major rivers throughout the world, with main regions being East Asia, the Caribbean, the Persian Gulf and the Red Sea, the Gulf of Mexico the Mediterranean, the Baltic Sea, the Maldives and coastal Indian Ocean. Many of these regions have a desperate need to improve transport effectiveness, which is linked to their economic growth.

1.2.3. Technical and economic feasibility

WIG craft is about high speed marine transportation, 100 knots, in comfort, without water contact, slamming shock, stress, wake, wash or seasickness. It is extremely fuel efficient. The ability to handle sea state of WIG crafts open potential usage in coastal, inter island and major rivers. Hundreds of millions of people living and working in locations these locations would benefit from WIG craft. WIG craft is about series/mass production of high speed marine craft at a manufacturing scale similar to the volume of the speedboat sector [3]. The market potential for WIG craft is huge that it is worth trying hard for. Low fuel consumption of high lift-to-drag ratio does not make WIG craft cheap. In the end, WIG is simply about being a fast, comfortable transport solution which asks little of other infrastructure investment. Making WIG craft commercially successful is a long journey, but it is worth taking.

WIG craft is a new product, a new market and a new industry. For it to be successful the technology must work, the Manufacturing company must be feasible, the Operating company must be feasible. It must also mean something to the ultimate customers/users in the civil and military markets. To an Engineer, the benefit of the WIG craft is in its power efficiency but to an investor, the benefit of the WIG is in its ability to make profit, which means lower operating cost. Thought WIG craft would be cheaper than an aircraft at one point, currently that is not the case. One needs to take into account the costs of research and development, wind tunnel testing, tank tests, safety assessment, certification procedure, general design costs ect. If all these costs were included in the price of one WIG, it would be more expensive than an aircraft [4]. In order to make WIG cheaper, mass production of ""identical"" vessels must take place. In order to make money in WIG craft, the key is to find the right market. WIG cratfs can be used to military or civil purposes. Why is it important to find the market and what does product mean to the market? There are benefits of zero water contact such as no sea motion or sea sickness, low fatigue for passenger, no wash, shallow water operations. Due to these benefits, WIG crfats would be ideal for civil market. As for the military application, though WIG crafts have benefits, the slowness of adaption of new technology is costing military to frown upon WIG crafts. Some day the WIG craft market is equal to the helicopter business. According to author, Graham Taylor, demand will outstrip supply of WIG craft at

least the first decade, giving manufacturers the opportunity to pick

their customer.

1.2.4. Critical mission requirement

A WIG craft, such as Hoverwing, need to have well-dimensioned planning surface and high power for take-off transition. The engineers involved with WIG research have focused on seeking methods to improve take-off performance and to reduce total installed power. The design challenge at cruising speed is aerodynamic stability and control due to its close proximity to the water surface.

1.3. Comparative study of similar airplanes

The mission capabilities of the similar airplanes include flying in Ground effect over water surfaces at high speeds. WIG technology is at a very early stage and covers wide range of craft configuration. The aircrafts listed in Table two are the Russian built aircrafts. Some other examples of 2-seater WIGs include Hydrowing2VT, SM-9, SM-10 and Strzh. Table three shows important design parameters of small scale WIG crafts.

Table 2. Russian WIG crafts

	SM 6	Orlyonok	KM	Spasatel	Volga 2
Mission	Small experimental modelof Orlynok	Transport	Experimental	Guided missile or/and rescueship	Passenger boat
Maximumtake off weight,t	26.42	140	544	upto400	2.7
Payload,t	1	20 Oct		upto100	0.75
Passenger modification		150		450	8
Dimensions,L/B/H m	31/14.8/7.85	58/31.5/16	92.3/37.6/22	73.8/44/19	11.6/7.6/3.7
Liftwing,Sm	73.8	307	662.5	500	44
AR,liftwing	2.81	3.07	2	3	1

Powerplant: Starting,typeand power	2TD9turbojet engine,2040kg thrustforeach	2NK 8 4K fanjet engine,10t thrusteach	8VD 1 NM turbojet engine, 11t thrust each	8NK 87 turbofan engine,12t thrusteach	2rotary piston engine,150 hpeach drvingtwo propellers
Cruising:typeand power	1AI 20 turboprop engine,4000hp	1NK 12MK turboprop engine, 15000hp	2VD 7KM turbojet engine, 11t thrust each	8NK 87 turbofan engine,13r thrust	
Cruisingspeed, km/h(knots)	290(157)	370 400 (200 215)	500(270)	370 400 (200 215)	120
Range,miles	497	1807.7	1242.74	2485	186
Waveheight3% (m)Takeoff/landing	upto1.0	1.5	5	2.5/3.5	0.5
Cruisingmode	upto1.5	nolimit	nolimit	nolimit	0.3
Staringdistance (miles)Oncalm water/In specification seastate	1.67/2.80	1.49 1.74/2.48 3.11	3.73	1.49 1.74/2.48 3.11	0.62
Startingtime(s) Oncalmwater/In specification seastate	50/75	80/150	130/200	80/150	70/50
Touchdowntostop (miles),Oncalm water/In specification seastate	0.75/1.12 1.67	0.75/1.05	1.92/2.80	0.75/1.05	0.50/0.62
Take offspeed, knots	113.39	118.79	151.19	118.79	43.2

Table 3. Important parameters of small scale WIG crafts

	DevelopmentseriesfortheVolgaandStrizh				
	SM 9	SM 10	Volga 2	Strzh E	Volga 1
Buildyear	1977	1985	1986	1991	1998

					1999
Length,ft	36.5	37.5	38	37.4	49
Mainwingspan, ft	32.32	25	25	21.6	41
Tainheight,ft	8.43	10.89	12.1	11.8	15.4
AR,maintail	0.9	0.9	0.9	3	
Crew+passengers	1+	1+	1+7	1+1	1+10
AUW,lbs	3500	4400	5400	3260	6600
Payload,lbs	1000	2000	2000	1000	
Thrust,t	300bhp	300bhp	300bhp	320bhp	300bhp
Enginestern					
Enginebow	2off ZMZ 4062 10	2off ZMZ 4062 10	2off ZMZ 4062 10	2off VAS 4133	2off 3M3 4062.10
Maximumspeed, knots	75.6	75.6	75.6	94.5	108
Cruisespeed, knots	65	65	65	81	65
Range,miles	n/a	186	500	311	186

Chapter 2. Weight Constraint Analysis

2.1. Database for takeoff weights and empty weights of similar airplanes

Table 4. Full size aircraft database of takeoff weights, empty weights and ranges

Aircraft	Payload weight, lbs	Takeoff weight, lbs	Range, mi	Empty Weight, lbs
SM-6	2000	52840	800	50840
Orlyonok	40000	280000	1300	240000
KM	-	1088000	2000	-
Spasatel	200000	800000	4000	600000
Volga-2	1500	5400	300	3900
SM-9	1000	3500	n/a	2500
SM-10	2000	4400	300	2500
Volga-2	2000	5400	500	3400
Strzh	1000	3260	300	2260
E-Volga-1	-	6600	300	-

Table four includes the payload weight, empty weight, takeoff weight and range of some of the WIG crafts that has been successfully tested.

2.2. Determinations of regression coefficients A and B

According to reference [5], the regression coefficients A and B for flying boats are 0.1703 and 1.0083, respectively. The regression coefficients A and B that were found using log-log chart were unattainable due to limited data provided for the WIG crafts. Therefore, during the calculations of skin friction drag above values for regression coefficients are used. The calculation of empty weight and fuel weight is shown in section 3.3.

2.2.1 Manual calculation of mission weights

<u>Step 1.</u> The mission payload weight was

assumed 16820 lbs <u>Step 2</u>. The mission TOW

was assumed to be 66333 lbs.

<u>Step 3.</u> The mission fuel weight was calculated to be 8286 lbs, with

25% fuel reserve weight.

<u>Step 4.</u>
$$W_{OEtent} = W_{TOguess} - W_F - W_{PL} \tag{1}$$

$$W_{OEtent} = 66333 -- 8286 -- 16820 = 41226 \text{ lbs.}$$

<u>Step 5.</u>
$$W_{Etent} = W_{OEtent} - W_{tfo} \tag{2}$$

W_{Etent} = 41226 lbs since crew weight is part of payload weight.

<u>Step 6.</u> To find W_E, the following equation was used:

$$\text{\ding{43}} \quad W_E = \text{inv } \log_{10} [(\log_{10} W_{TO} - A) / B] \tag{3}$$

Where the regression coefficients A and B were found to be 0.1703 and 1.0083.

$$B \log_{10} W_E = \log_{10} W_{TO} - A$$

$$\log_{10} W_E + A = B\log_{10} W_{TO}$$

$$\text{Æ } W_E = \text{inv } \log_{10} [(\log_{10} W_{TO} - A) / B] = 41033 \text{ lbs}$$

Substituting the values of A and B into the previous equation gives us

a W_E of 41033 lbs for a W_{TO} = 66333 lbs.

<u>Step 7.</u> The W_{Etent} and W_E values are within the 0.5% tolerance, the

calculations would not need to be repeated.

2.2.2 Calculation of mission weights using the AAA program

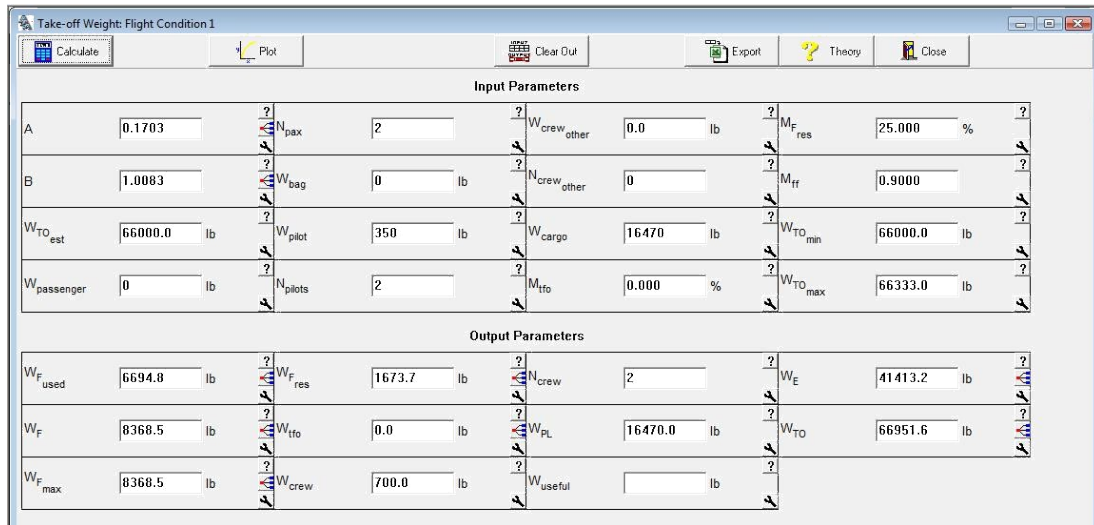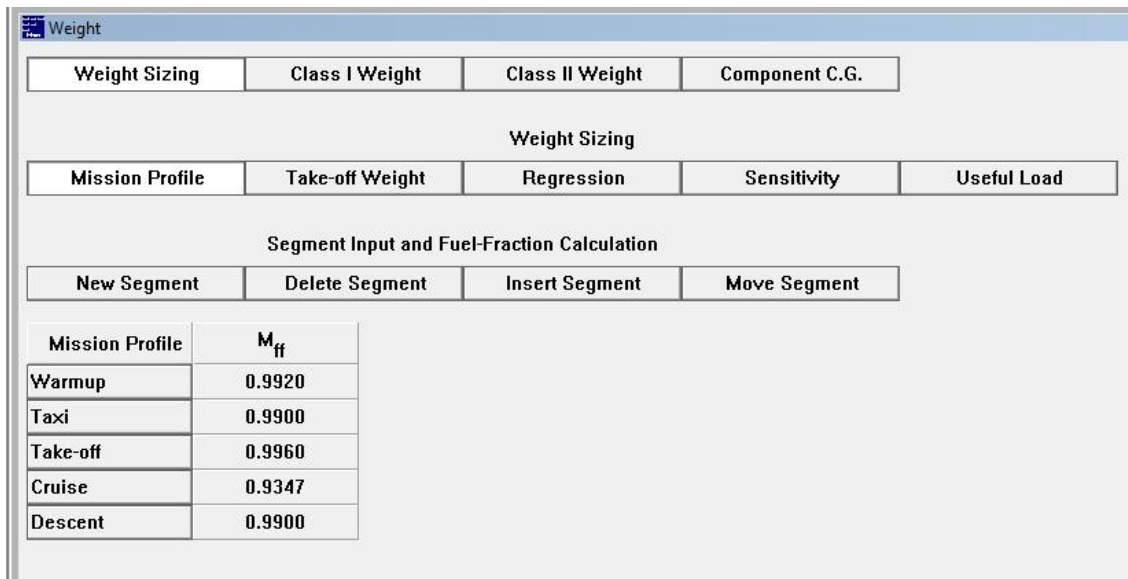Figure 2. Mission weights from AAA program

Figure 3. Mission fuel fractions

2.3. Takeoff weight sensitivities

2.3.1. Manual calculation of takeoff weight sensitivities
To calculate the takeoff weight the following equation was used:

$$\frac{3}{4} \qquad \log_{10} W_{TO} = A \; B \log_{10} (C \; W_{TO} - D) \qquad\qquad (4)$$

where A and B were calculated in section 2.2 to be 0.1703 and 1.0083.

14

To calculate C:

¾ $C = \{1 - (1 - M_{res})(1 - M_{ff}) - M_{tfo}\}$ (5)

with M_{res} and M_{tfo} can be assumed to
be zero.
To calculate
D:

¾ $D = W_{PL} + W_{crew} + W_{Pexp}$ (6)

To calculate M_{ff}, the following equation needed to be
used:

¾ $M_{ff} = \left[\dfrac{W_1}{W_{TO}} \quad \dfrac{W_2}{W_2} \quad \dfrac{W_3}{W_2} \quad \dfrac{W_4}{W_3} \quad \dfrac{W_5}{W_4} \quad \dfrac{W_6}{W_5} \quad \dfrac{W_7}{W_6} \quad \dfrac{W_8}{W_7} \right]$ (7)

$M_{ff} = [0.992 + 0.990 + 0.996 + 0.985 + 0.956876 + 0.99604 + 0.990 + 0.990] = 0.900006$

¾   Therefore $C = \{1 - (1 - M_{res})(1 - M_{ff}) - M_{tfo} = 1 - (1 - 0.900006)$
    $= 0.900006$

¾   and $D = W_{PL} = 16820$ lbs

This leads the takeoff weight to be calculated with:

$\log_{10} W_{TO} = A$

$B \log_{10} (C\ W_{TO} -- D) = 0.1703$

$$1.0083\log_{10}(0.900006\ W_{TO} -- 16820)$$

$$Æ\ W_{TO} = 10^{(0.1703 \cdot 1.0083\log_{10}(0.900006 W_{TO} - 16820)}$$

$$Æ\ W_{TO} = 69343\ lbs$$

Assuming:

$W_{TO} = 66333$ lbs

$W_E = 41033$ lbs

$A = 0.1703$

$B = 1.0083$

$C = 0.90006$

$D = 16820$

$$\frac{\partial W_{TO}}{\partial W_E} = BW_{TO}[inv\log_{10}\{\log_{10} W_{TO} - A/B\}]^{-1}$$

$$\frac{\partial W_{TO}}{\partial W_E} = 1.63$$

$$\frac{\partial W_{TO}}{\partial W_{PL}} = BW_{TO}\{D - C(1-B)W_{TO}\}^{-1}$$

$$\frac{\partial W_{TO}}{\partial W_{PL}} = 3.86$$

2.3.2. Calculation of takeoff weight sensitivities using the AAA program
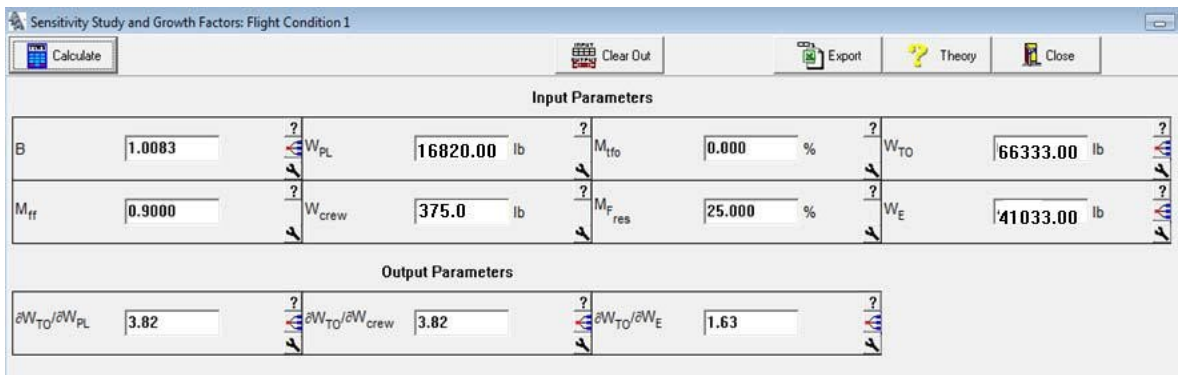

Figure 4. Results of takeoff sensitivities using AAA
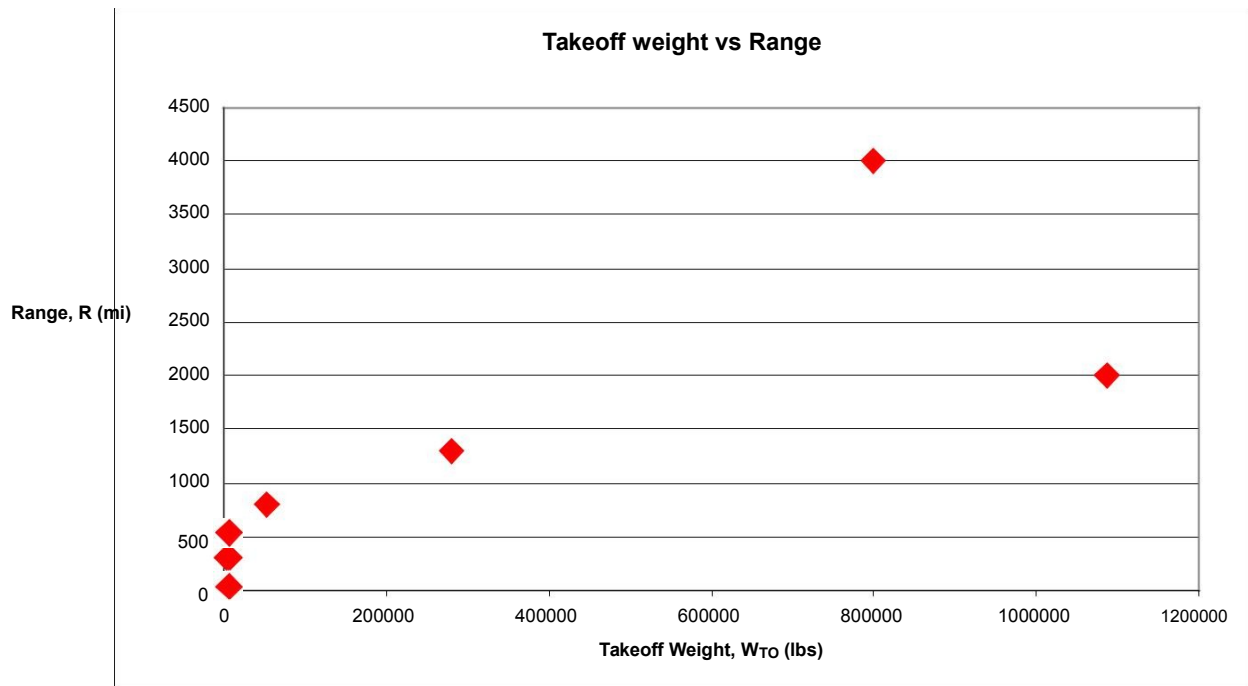
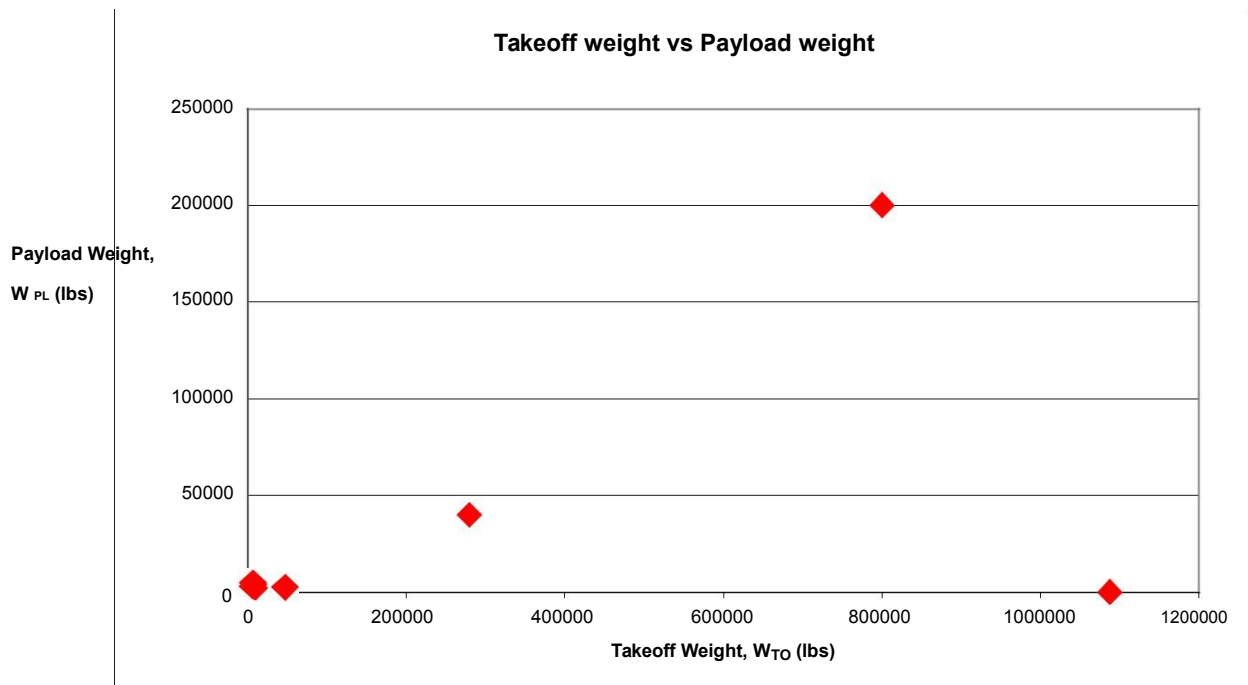## 2.4. Trade studies

Figure 5. Takeoff weight vs Range

Figure 6. Takeoff weight vs. Payload weight

Many of the mission weights such as the mission payload weight, take-off weight, and fuel weight were assumed based on the design of Hoverwing 80. The W_{OEtent} was calculated to be 41226 lbs, which by itself seems like a reasonable weight for the WIG craft. An empty weight of 41033 lbs was calculated with the regression coefficients from a Reference [5]. Since the data on WIG crafts is very limited and very scattered on the graphs, the log-log chart method was not achievable. Since the method described in reference [5] results are within the 0.5% tolerance of the W_{OEtent}, the calculations would not need to be repeated.

When the mission weights were calculated in the AAA program reliable results were obtained. The regression coefficients from reference [5] were entered and the results showed empty weight and fuel weight to be very similar to those calculated manually. The growth factors from AAA suggest that for every 3.82 lbs of payload weight that is added, one pound of takeoff weight can be added. The crew growth factor is not applicable to this project. The empty weight growth factor suggests that for every 1.63 lbs of empty weight, the takeoff weight increases by one pound. These growth factors are encouraging because that means a higher ratio of payload to empty weight. When the growth factors were calculated by hand, the results were with 0.5% error margin. The empty weight sensitivity has 0% error when manually calculated.

The range of this craft is assumed to be 497 miles. According to TOP 25, endurance of this craft has to be about 30 minutes during day time. This craft is assumed to fly only during day time, night time endurance has not been taken into consideration. The power required to operate this craft is higher than those listed in reference [5], therefore the

propeller will have be chosen. The parameter such as propeller efficiency might not be

available.

Chapter 3. Performance Constraint Analysis

3.1. Stall speed

An average max lift coefficient value of 1.4 was assumed. The calculations were performed for the max weight of 66333 lbs as well as a safer goal weight of 50000 lbs. The wing area is already known to be 3175 ft^2. The density of the air at sea level is 0.00237 slugs/ft^3.

W/S = 66333 / 3175 = 20.89 lb/ft^2

$$V_s = \sqrt{\dfrac{2\dfrac{W}{S}^{0.5}}{U C_{L\max}}} = 105 \text{ knots} \tag{8}$$

These equations were repeated for a weight of 50000 lbs, which has a wing loading W/S = 16 lb/ft^2 therefore a value of V_{SL} = 96 knots. The lower the weight was, the lower the stall speed. A lower stall speed is more favorable because it provides a lower landing speed therefore a lower landing distance. This parameter is not applicable for Hoverwing since Hoverwing will be flying very close to surface; no stalling conditions are taken into consideration. It is calculated to estimate landing distance. Since this parameter is not applicable for Hoverwing, AAA analysis was not taken into consideration.

3.2. Takeoff distance

The takeoff wing loading was taken as:

$(W/S)_{TO} = 66333lbs / 3175sqft = 20.89 lbs/ft^2$

$_1$ = 1 since the pressure at sea level in ratio of pressure at sea level is very close to 1.

$$TOP_{25} = (W/S)_{TO}/\{ _1 C_{L\ MAXTO}\ (T/W)_{TO}\} = 114.7 \text{ lbs}^2 / \text{ft}^2\text{hp} \tag{9}$$

S_{TOFL} = 37.5 TOP$_{25}$ =4304 ft

This takeoff distance was unacceptable therefore working backwards starting with a

S_{TOFL} of 3280 ft (the takeoff constraint), the takeoff parameter resulted in a value of

87.47 lbs^2 / ft^{2}hp. The equation became:

87.47 lbs^2 / ft^{2}hp = $(W/S)_{TO}/\{ \iota C_{L\ MAXTO}\ (T/W)_{TO}\}$

 By using different C_Ls ranging from 1.6 to 2.2, and varying the values of $(W/S)_{TO}$ versus

$(T/W)_{TO}$, a graph was produced to see how each of the three variables affected

each other:

Table 5. Calculated results of thrust-to-weight ratio versus wing loading as a function of
varied lift coefficient

|	C_{LMAXTO} = 1.6	C_{LMAXTO} = 1.8	C_{LMAXTO} = 2.0	C_{LMAXTO} = 2.2
(W/S)$_{TO}$	**(T/W)$_{TO}$**	**(T/W)$_{TO}$**	**(T/W)$_{TO}$**	**(T/W)$_{TO}$**
5	0.03573062	0.031760551	0.028584496	0.025985905
10	0.071461239	0.063521102	0.057168992	0.05197181
15	0.107191859	0.095281653	0.085753487	0.077957716
20.89	0.149282529	0.132695581	0.119426023	0.108569112
25	0.178653099	0.158802754	0.142922479	0.129929526
30	0.214383718	0.190563305	0.171506975	0.155915431
35	0.250114338	0.222323856	0.20009147	0.181901337
40	0.285844958	0.254084407	0.228675966	0.207887242
45	0.321575577	0.285844958	0.257260462	0.233873147
50	0.357306197	0.317605509	0.285844958	0.259859052
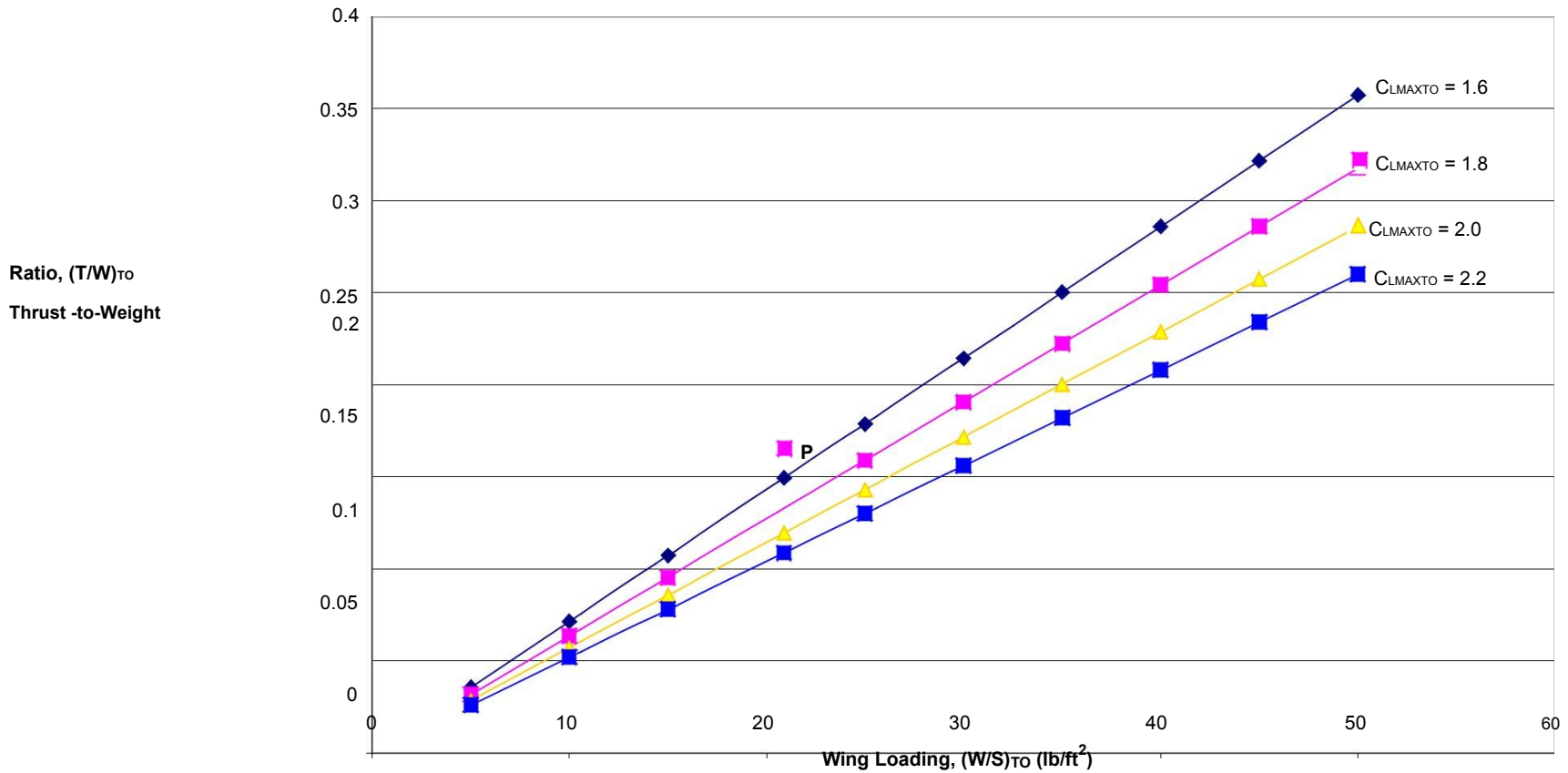
Figure 7. Thrust-to-weight ratio vs Wing loading as a function of varied lift coefficient

By using different C_{DS} at C_L ranging from 1.6 to 2.2, and varying the values of $(W/S)_{TO}$ versus $(W/P)_{TO}$, a graph was produced to see how each of the 3 variables affected each other using below equation

$$V = 77.3 \; \{Ş_P \, (W/S)/ı \, C_D \, (W/P)\}^{1/3} \tag{10}$$

Using $V = 125$ knots, $Ş_P = 0.75$, and $ı = 1$, equation becomes

$$(W/P) = \{0.000098 \, (W/S)\}/C_D$$

Table 6. Calculated results of wing loading versus power loading

|	$C_L = 1.6$	$C_L = 1.8$	$C_L = 2.0$	$C_L = 2.2$
(W/S)$_{TO}$	**(W/P)$_{TO}$**	**(W/P)$_{TO}$**	**(W/P)$_{TO}$**	**(W/P)$_{TO}$**
5	0.000685	0.0004283	0.000281	0.000192305
10	0.001369	0.0008566	0.000563	0.00038461
15	0.002054	0.0012849	0.000844	0.000576915
20	0.002738	0.0017132	0.001125	0.00076922
25	0.003423	0.0021415	0.001407	0.000961525
30	0.004108	0.0025698	0.001688	0.00115383
35	0.004792	0.0029981	0.001969	0.001346135
40	0.005477	0.0034264	0.002251	0.001538441
45	0.006162	0.0038547	0.002532	0.001730746
50	0.006846	0.004283	0.002813	0.001923051
55	0.007531	0.0047113	0.003095	0.002115356
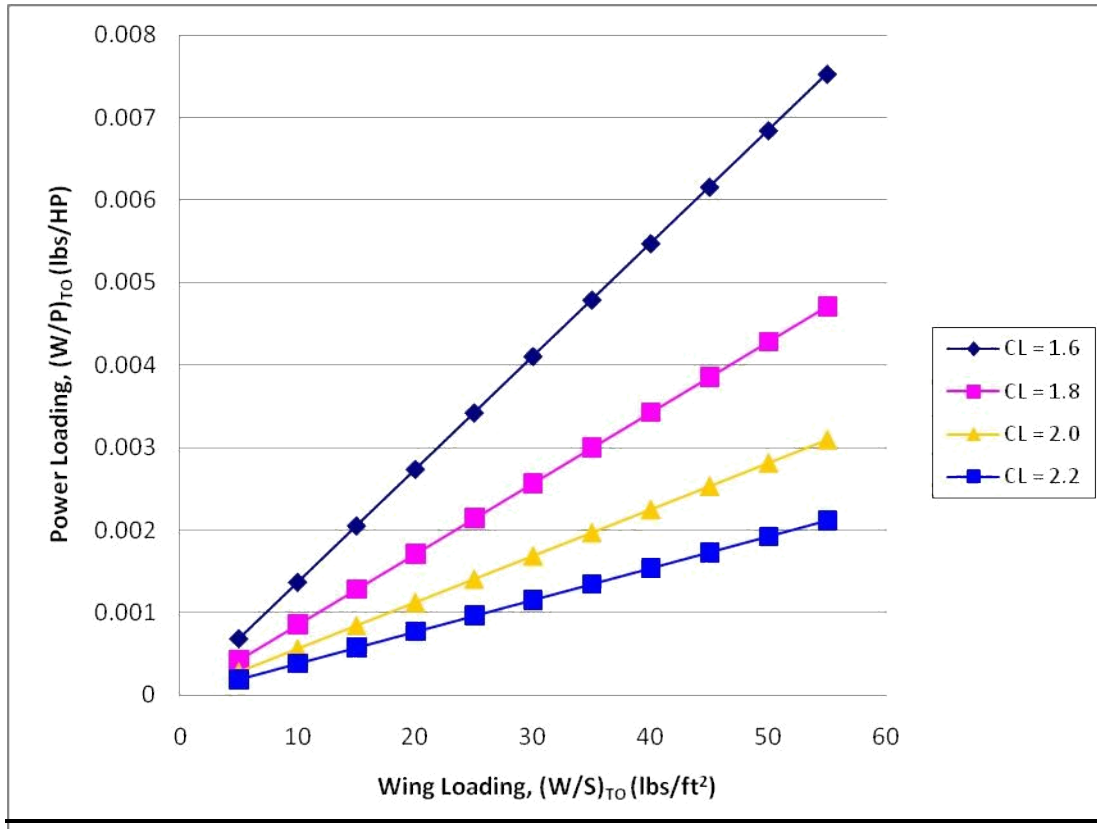
Figure 8. Power loading vs Wing loading as a function of varied lift coefficient

For Hoverwing, the C_L of 1.8 was chosen. It is seen from the graph that lower C_L causes lower wing and power loadings. It is desirable to have lower wing loadings as to have lower speeds before stall occurs. Also a lower power loading is desired so the aircraft could have better performance. Therefore, a point should be chosen that is closest to the lower left corner but preferably with a medium to high C_L. In this case, C_L of 1.8 was chosen with wing loading of 21 to have better power loading, which gives the take off power required to be about 6700 HP.

Power required to cruise can be found using below equation [5]:

$$P_{req} \quad \frac{1}{2} U V^3 S C_{D,0} \quad \frac{W^2}{0.5 U V S} (\frac{1}{S e A})$$
(11)

Where, d_0 is 0.00237slugs/ft^3, velocity is 125 knots, S is 3175 ft^2, W is 66333 lb, AR

is 3.45, e is 0.88 and $C_{D,0}$ is 0.004. Plugging all the values in the above equation gives

an answer of 1.06 x 10^6 ft-lb/sec, which is about 3300 HP. According to this data,

Hoverwing will need about 3300 HP during cruise.

3.3. Landing distance

The FAR landing field length is defined as the total landing distance divided by 0.6. This

factor of safety is included to account for variations in pilot techniques and weather

conditions. It is assumed that Hoverwing will have a landing distance of 3280 ft.

$$V_A = (S_L / 0.3)^{1/2} = 88 \text{ knots} \tag{12}$$

$$V_{SL} = V_A/1.3 = 104/1.3 = 67 \text{ knots} \tag{13}$$

Compared to the stall speed calculated in section 2.1 of 66 knots, this value will allow us

to come to a full stop within 3280 feet.

Figure 9. AAA calculation for landing requirement

The landing distance of 3167 ft is required to have a safe landing, which is seen from

figure 8. Wing loading of 96 lb/ft^2 is calculated by AAA. This data is acceptable as long

as the wing loading is under 100 lb/ft^2.

3.4. Drag polar estimation

To calculate the drag polar C_{D_o}, the regression line coefficients for takeoff weights versus wetted area were acquired through reference [5]. The values of c and d for flying boats were found to be 0.6295 and 0.6708. The W_{TO} is 66333 lbs.

$$\log_{10} S_{wet} = c + d \log_{10} W_{TO} \tag{14}$$

$$\log_{10} S_{wet} = 3.864$$

To find the equivalent parasite area f, $\log_{10} S_{wet} = 1.9716$ was substituted into the following equation:

$$\log_{10} f = a + b \log_{10} S_{wet} \tag{15}$$

Skin friction coefficient was found using the graph 3.21c in reference [5]. The correlation coefficients a and b were found through table 3.4 from reference [5] to be -2.3979 and 1.

$$f = 29.24$$

The equivalent parasite area and the wetted area S_{wet} are related in the following way:[3]

$$C_D = C_{D,0} + \frac{C_L^2}{S A e} \tag{16}$$

$$\text{where } C_{D,0} = \frac{f}{S} \tag{17}$$

By substituting the equivalent parasite area $f = 29.24$ into the zero-lift drag coefficient equation:

$$C_{D,0} = \frac{f}{S} = 0.004$$

Substitute this information in C_D equation to get following drag polar,

$$C_D = C_{D,0} + \frac{C_L^2}{S A e} = 0.004 + \frac{1.4_2}{S * 3.45 * 0.85} = 0.212$$

Low speed, clean: $C_D = 0.004 + 0.109\, C_L^2$

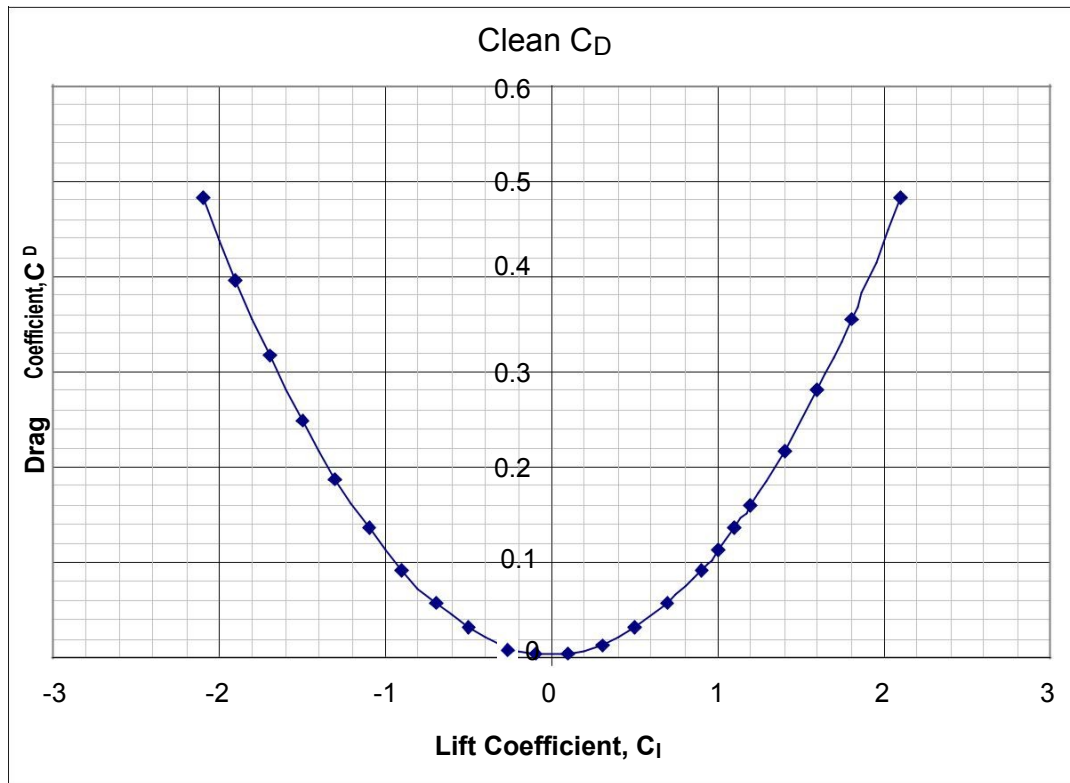Figure 10. Drag polar graph

According to figure 10, the higher the lift coefficient, the higher the drag and parasite drag coefficients will be. It is desirable to choose a higher lift coefficient while keeping the parasite and drag coefficients low. It is also seen that during takeoff and landing, the drag is higher. The lift coefficient of 1.8 is chosen for Hoverwing.
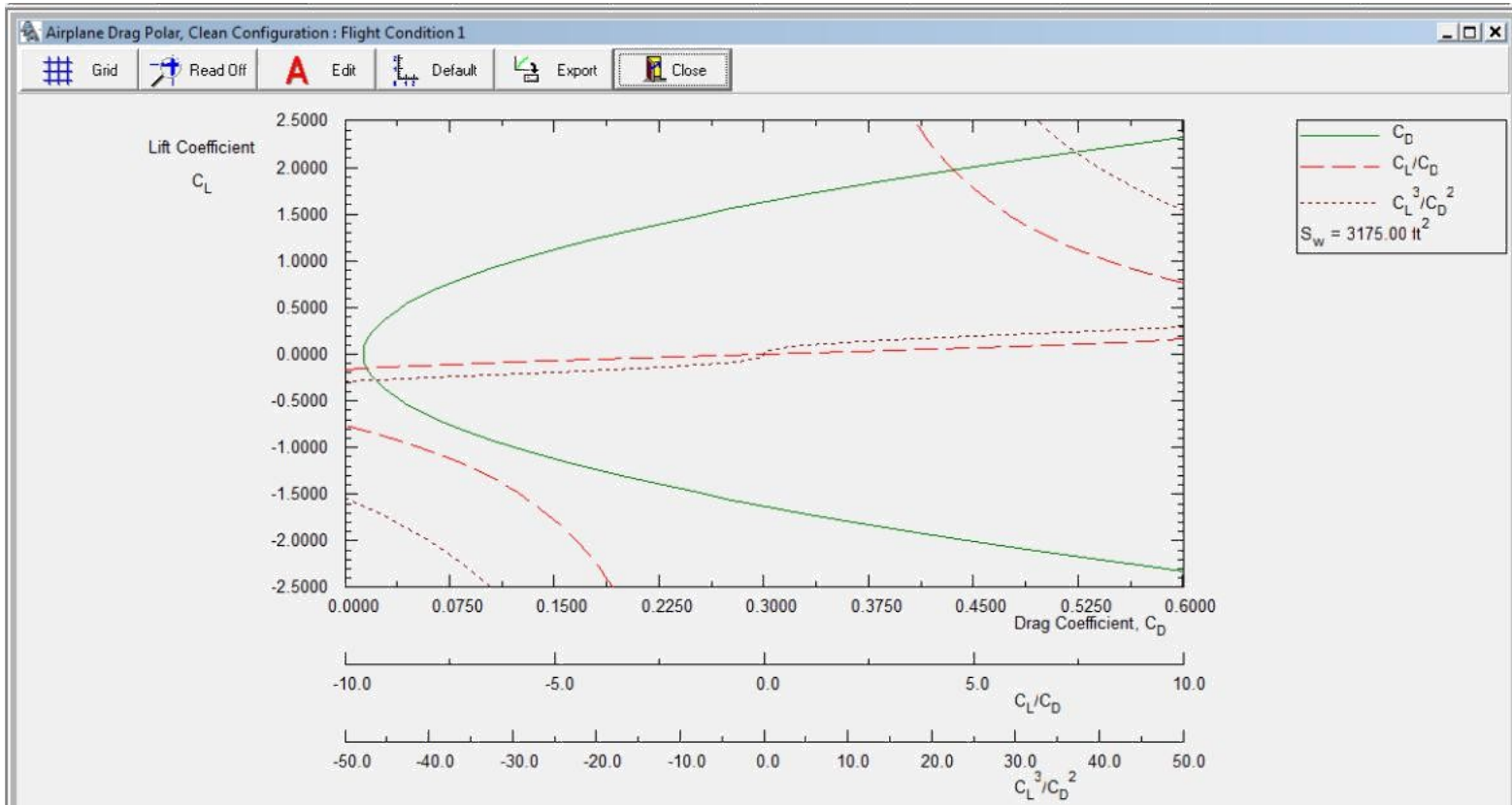
Figure 11. Clean drag polar

The drag polar data from AAA were similar to data obtained by excel sheet. Since

Hoverwing will not have any lateral control surfaces or landing gear, only clean drag

calculations were made. The data achieved from AAA has similar value at C_l of 1.8,

which is 0.360. According to figure 9 and 10, the higher the lift coefficient, the higher the

drag and parasite drag coefficients will be.

In order to get the skin friction coefficient, the graph for military aircraft was chosen

from reference [5]. The aircraft that has the weight closest to Hoverwing was taken into

consideration. Therefore, the manual calculations are very reliable for drag polar.

The matching plot could not be obtained from AAA. Hoverwing does not have flaps or

slats, so when data was entered into AAA, it only produced blank graphs with no results.

3.5. Speed constraints

Table 1 specifies a cruise speed of 125 knots at 15 ft. The low speed, clean drag polar for

the proposed airplane is given by,

$C_D = 0.004 + C_L{}^2/9.20$, for A = 3.45 and e = 0.85

The following equation satisfies the cruise speed sizing for FAR 25 airplanes,

$$(T/W)_{reqd} = \frac{C_{D_0} \, qS}{W} = \frac{W}{qSSA \, e}$$ (18)

By substituting the values in above equation, we

get $(T/W)_{reqd} = 4.92/(W/S) + (W/S)/9.20$

Table 7. Data for takeoff speed sizing

(W/S)$_{TO}$	(T/W)$_{TO}$
15	0.18
20	0.17
25	0.16

30	0.15
35	0.13
40	0.12
45	0.11
50	0.10

Table 7 shows the data for cruise speed sizing for the proposed design. The ratio of thrust at V = 125 knots at 15 ft to that sea level, static is roughly 0.1. This is based on typical turbofan data for this type of airplane.
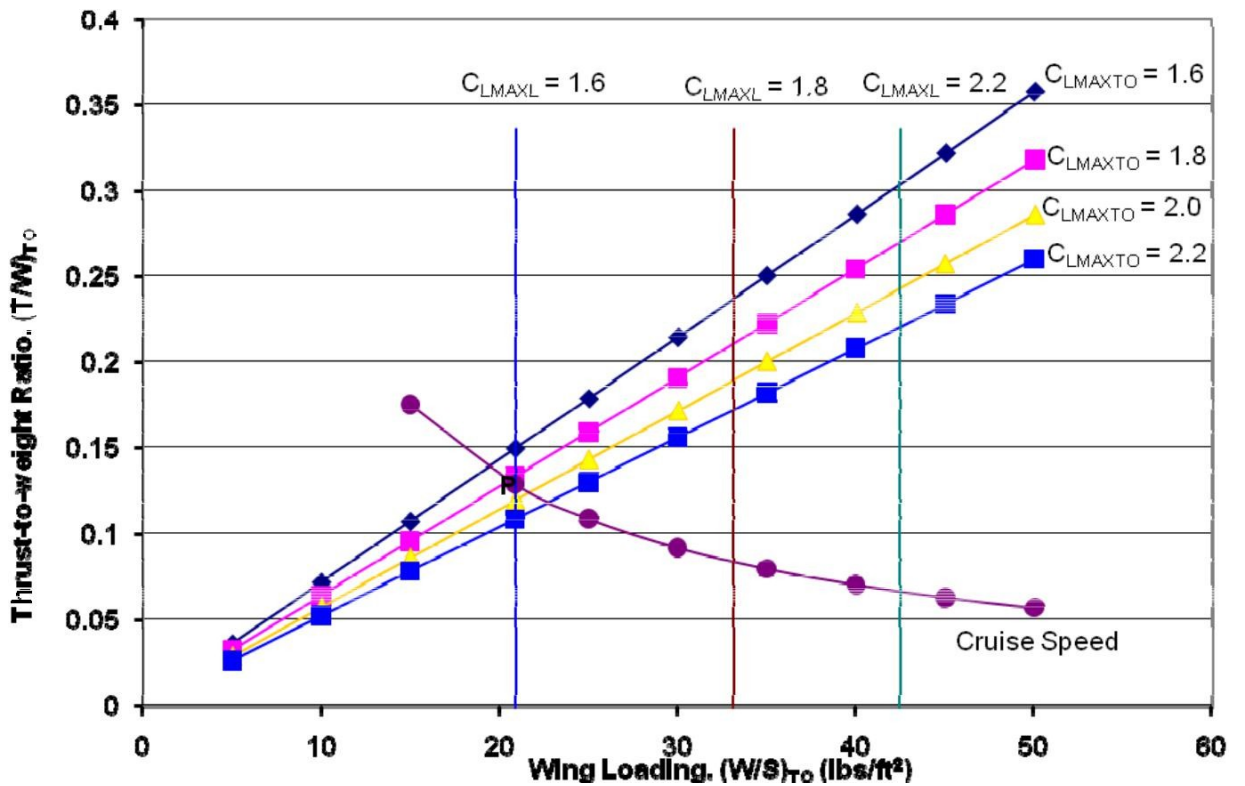
3.6. Matching graph

Figure 12. Matching results for sizing of a hoverwing

From above graph, it is seen that point P is accepted as a satisfactory match point for Hoverwing. The airplane characteristics are summarized as follows:

Take-off weight: W_{TO} = 66,333 lbs

Empty weight: $W_E = 41{,}033$ lbs

Fuel weight: $W_F = 8286$ lbs

Take-off: $C_{L,maxTO} = 1.8$

Landing: $C_{L,maxL} = 1.6$

Aspect ratio: 3.45

Take-off wing loading: $(W/S)_{TO} = 20.89$ lb/ft^2

Wing area: $S = 66333/20.89 = 3175$ ft^2

Take-off thrust-to-weight ratio: $(T/W)_{TO} = 0.133$

Take-off thrust: $T_{TO} = 8{,}822$ lbs

Chapter 5. Fuselage Design

The ""Hoverwing"" will have a catamaran empennage configuration with a T-tail since it is safer and easier to operate in water. A catamaran empennage configuration helps to build a static air cushion by diverting some of the propeller slip-stream, which creates about 80% of the crafts weight as lift while the speed is 0. Below is the configuration of the fuselage in exact dimensions. The configuration on the left is bottom view and the configuration on the right is the side view. Hoverwing flies very close to surface, therefore the cabin does not need to be pressurized. The seating arrangements are not being discusses since this craft is designed to carry cargo only.
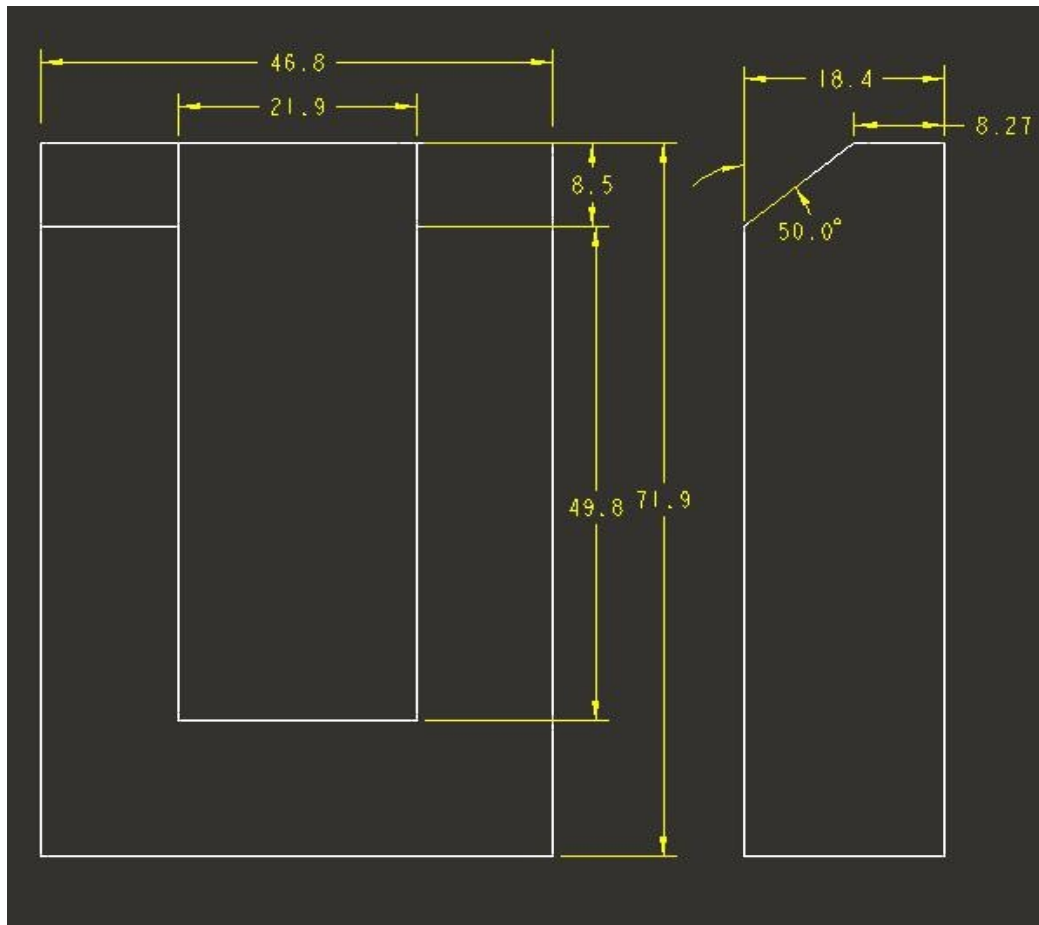
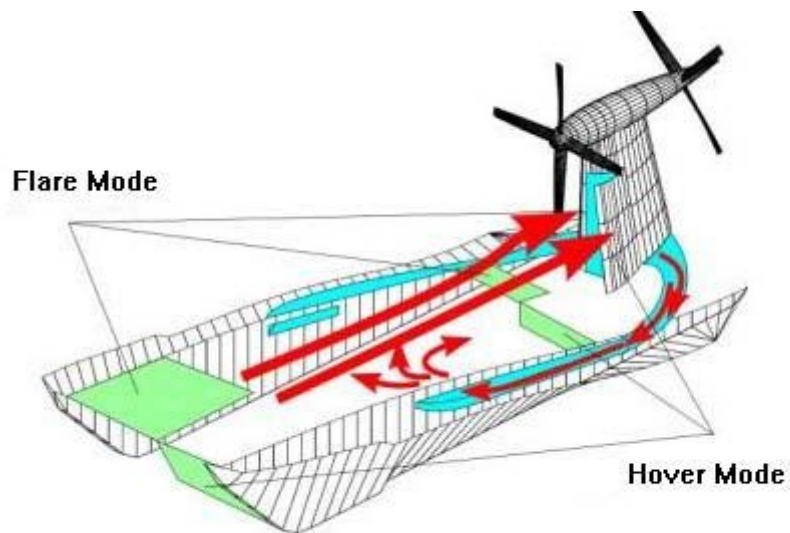Figure 13. Design of the fuselage of hoverwing

Figure 14. Catamaran fuselage [4]

Chapter 6. Wing Design

6.1. Wing platform design

The wing configuration will be the conventional one as there were significant problems with the other wing configurations, which would make the design and construction process more difficult as well as the piloting.

The overall structural wing configuration will be a reverse delta wing. The disadvantage of delta wing, especially in older tailless delta wing designs, are a loss of total available lift caused by turning up the wing trailing edge or the control surfaces and the high induces drag of this low aspect ratio type of wing. This is the reason that causes delta winged aircraft to lose energy in turns, a disadvantage in aerial maneuver combat and dogfighting. Since the Hoverwing will be flying very close to water surfaces, this disadvantage will have very little to no impact in WIG craft performance.

A reverse delta will be stronger than a similar swept wing, as well as having much more internal volume for fuel and other storage. Another advantage is that as the angle of attack increases the leading edge of the wing generates a vortex which remains attached to the upper surface of the wing, giving the delta a very high stall angle.

Other advantages of the delta wing are simplicity of manufacture, strength, and substantial interior volume for fuel or other equipment. Because the delta wing is simple, it can be made very robust. It is easy and relatively inexpensive to build. The reverse delta wing also has a significant advantage in the longitudinal stability of the craft which is extremely important in WIG crafts.

The reverse delta wing has a large aerodynamic center shift as Mach number increases from subsonic to supersonic. This will not be a problem for Hoverwing due to expected low speeds of the flight. Subsonic wind-tunnel tests were conducted with a variety of leading- and trailing-edge flap planforms to assess the longitudinal characteristics of a reverse delta wing. The experimental data show that leading-edge flaps are highly effective at increasing maximum lift and decreasing drag at moderate angles of attack. Trailing-edge flaps were up to 90% as effective as delta wing flaps in generating untrimmed lift increments.

A low-wing configuration provides extreme ground effect while taking off and landing while also providing an easier maneuvering capability during both events. It can also be used to step out onto for hoverwing exits. Other advantages include easier access for maintenance and cabin. Because of low-wing configuration, it provides better flexibility on wing span yielding better cruise performance.

The wing area and the aspect ratio of the Hoverwing are 3175 ft^2 and 3.45, respectively. These values were calculated in previous reports. The taper ratio of the wing is chosen to be 0.47 for the Hoverwing. Tapering a wing gives a higher aspect ratio, root chord to tip chord over the span thus being more efficient. The smaller sections towards the tip require less structure, both due to size and the reduced stress on the structure. The taper ratio itself is usually governed by the performance expected from the plane.

The Hoverwing will have a dihedral angle of 2°. Dihedral is added to the wings to increase the spiral stability and dutch roll stability. A

major component that affects the aircraft''s effective dihedral is the

wing location with respect to the fuselage. Having

dihedral also increases the ground clearance of the wings. This would be a very important factor when flying in rough seas where waves are higher. It is seen that the dihedral makes an aircraft more stable.
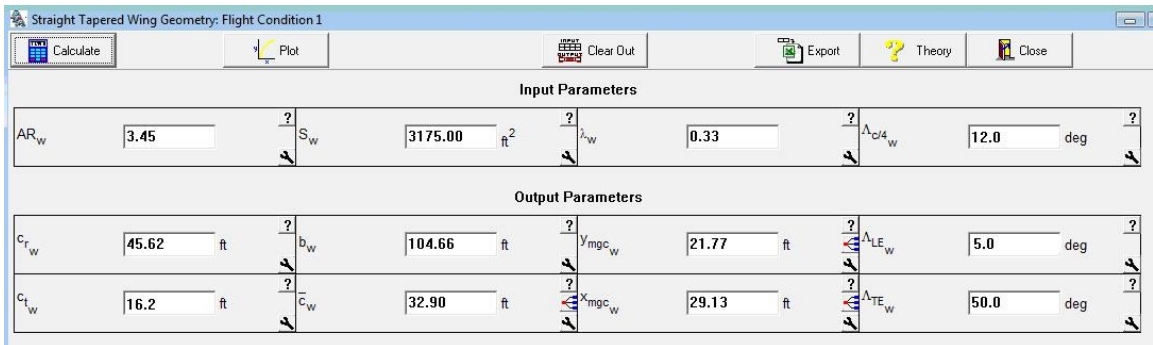

Figure 15. Straight tapered wing geometry

AAA calculated the tip chord to be 16.2 ft and root chord to be 45.6 ft, which will be used to design the main wing. The geometry of wing could not be obtained from AAA since AAA did not calculate for reversed delta wing. This wing configuration is very unique; therefore AAA plot was not taken into consideration.

6.2. Airfoil selection

The Hoverwing will be fitted with a Clark Y airfoil Clark. The airfoil has a thickness of 11.7 percent and is flat on the lower surface from 30 percent of chord back. The flat bottom simplifies angle measurements on the propellers, and makes for easy construction of wings on a flat surface. For many applications the Clark Y has been adequate; it gives reasonable overall performance in respect to its lift-to-drag ratio, and has gentle and relatively benign stall characteristics. The depth of the section lends itself to easier wing repair. The higher the lift coefficient, the more it will prevail over the effects of the drag coefficient. Due to the expected lower velocities of flight, the effects of drag are not

expected to be too significant therefore increasing the benefits of a higher lift. The C_l vs

C_d curve for Clark y airfoil is shown in Figure 16. The XFLR software was unable to

calculate the curve for the Reynolds number of 1 x 10^7. Therefore, the Reynolds number

of 6 x 10^6 Lift coefficient vs Drag coefficient curve is shown in figure 17 [6].

 The Hoverwing will have a 4-degree incidence angle. This helps keep the fuselage level.

It is necessary as it allows the fuselage and other components to cause as little drag as

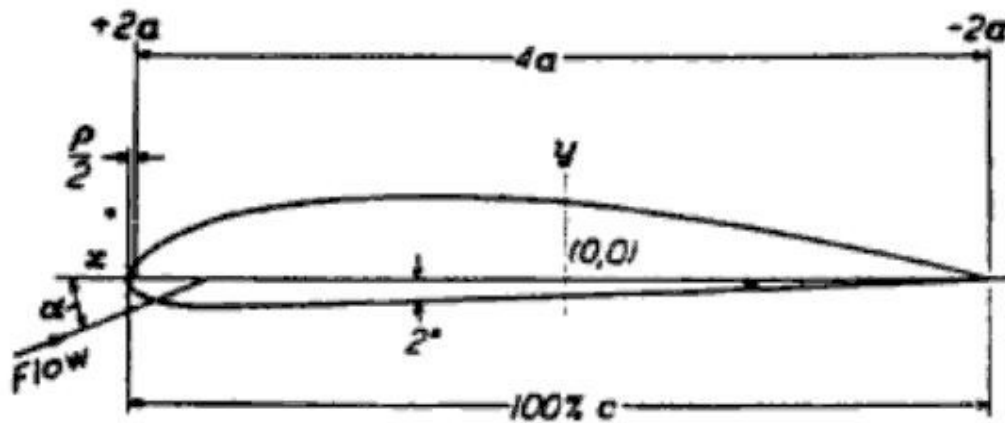possible. It also allows the airplane to takeoff earlier.

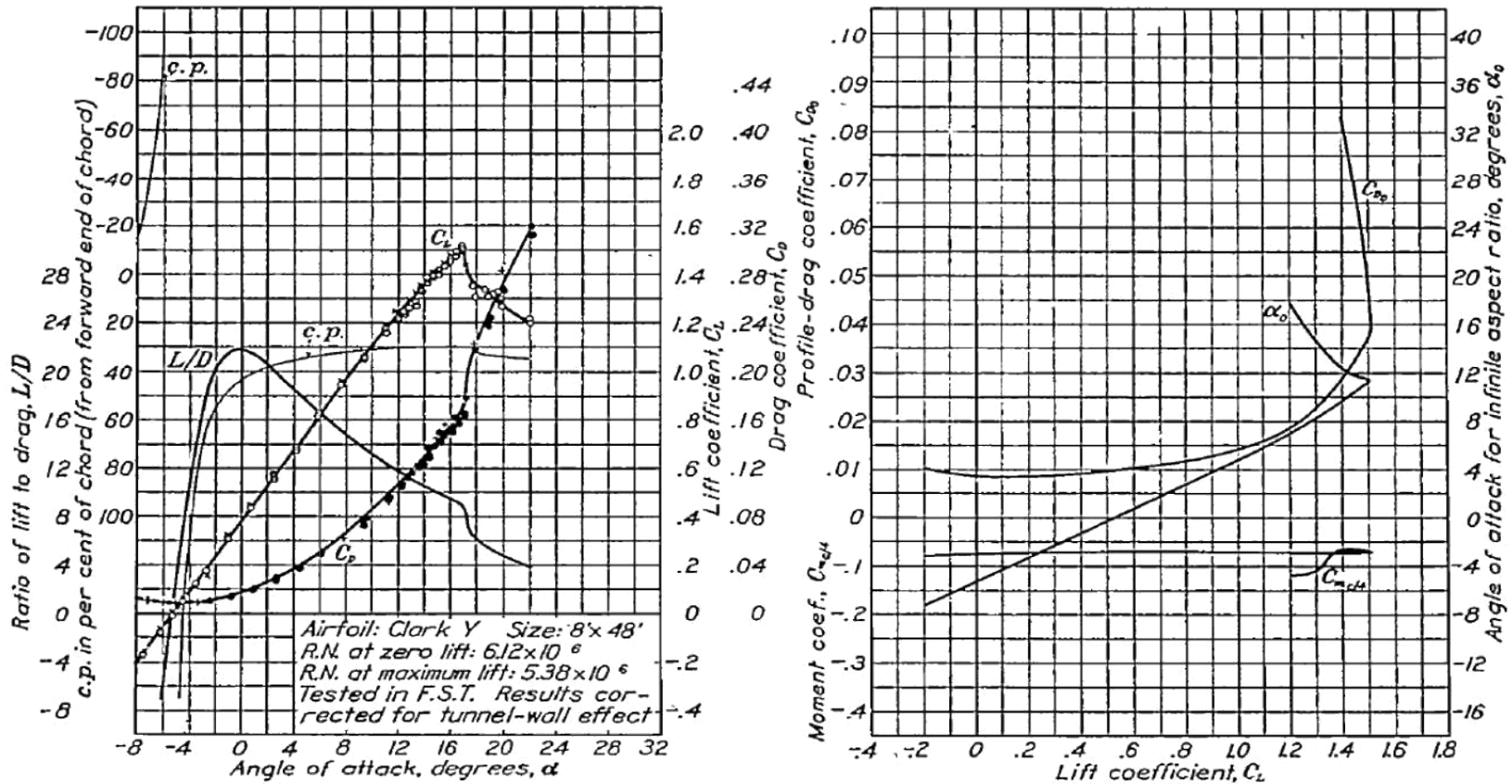Figure 16. Geometry of Clark Y airfoil [6]

FIGURE 8.—Characteristics of the 8 by 48 Clark Y airfoil at a Reynolds Number of about 6,000,000.

Figure 17. Lift coefficient vs Drag coefficient curve for Clark Y airfoil [6]
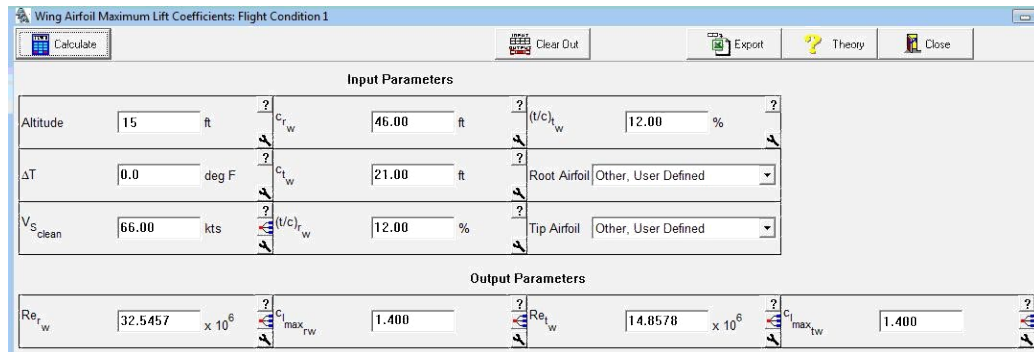
38

Figure 18. Calculation of lift coefficient using AAA program

When the values were entered into the AAA program, the Reynold''s number resulted in value of 3.2×10^7. The $C_{l,max}$ values were entered in AAA program manually since the

AAA program would not calculate the $C_{l,max}$ for Clark Y airfoils since it only includes the $C_{l,max}$ data for NACA airfoils.

6.3. Design on the lateral control surfaces

The Hoverwing will not have any ailerons, spoilers, flaps, slats or airbrakes. Hoverwing is designed to fly very close to the water surface with zero to minimum amount of turning. Therefore, there is no need to have ailerons or any other control surfaces on the wing. The Hoverwing will have tip tanks and winglets. Wing tip tanks can act as a winglet, store fuel at the center of gravity, and distribute weight more evenly across the wing spar. The wingtip vortex, which rotates around from below the wing, strikes the cambered surface of the winglet, generating a force that angles inward and slightly forward, analogous to a sailboat sailing close hauled. The winglet converts some of the otherwise-wasted energy in the wingtip vortex to an apparent thrust. The winglets will be 15 ft in height, the root chord 21 ft, and the tip chord 8 ft. It will be located at a 56° angle from the main wing.

The mean aerodynamic center (MAC) of the wing was found using by following equation [7]:

$$MAC = \frac{S}{2} \int^{b/2} C^2 \, dy \qquad (19)$$

Since the wing of the Hoverwing is a tapered wing, the location of the MAC will be computed using above equation. However, the chord of the tapered wing can be calculated by below equation:

$$c(y) = \frac{2S_w}{(1+\lambda)b} \left[1 - \frac{2(1-\lambda)}{b} y\right) \qquad (20)$$

The taper ratio of the Hoverwing will be 0.47 as mentioned in section 6. From the above equation, the chord of the wing is 32 ft. Using this value, the Reynolds number was calculated to be 2.23 x 10^7. The MAC of the wing will be at ¼ chord of the MAC. The coordinates of the MAC of the wing will be at 8 ft in from the leasing edge and 32 ft. The Hoverwing will have reverse delta wings. Reverse delta wings have the same effect as delta wings in terms of drag reduction, but has other advantages in terms of low-speed handling where tip stall problems simply go away. In this case the low-speed air flows towards the fuselage, which acts as a very large wing fence. Additionally, wings are generally larger at the root anyway, which allows them to have better low-speed lift. Winglets will be added to the tips of the wings as to reduce induced drag. A winglet with a sharp corner with respect to the wing will be used, as it is easiest to construct. Unfortunately, this choice does create problems. By being located in the pressure rise region of the wing, winglets help move the pressure rise of the winglet behind the trailing

edge. Because the winglet causes a favorable pressure gradient, it cancels out some of the

wing''s pressure rise.

6.4 CAD drawing of a wing and a winglet
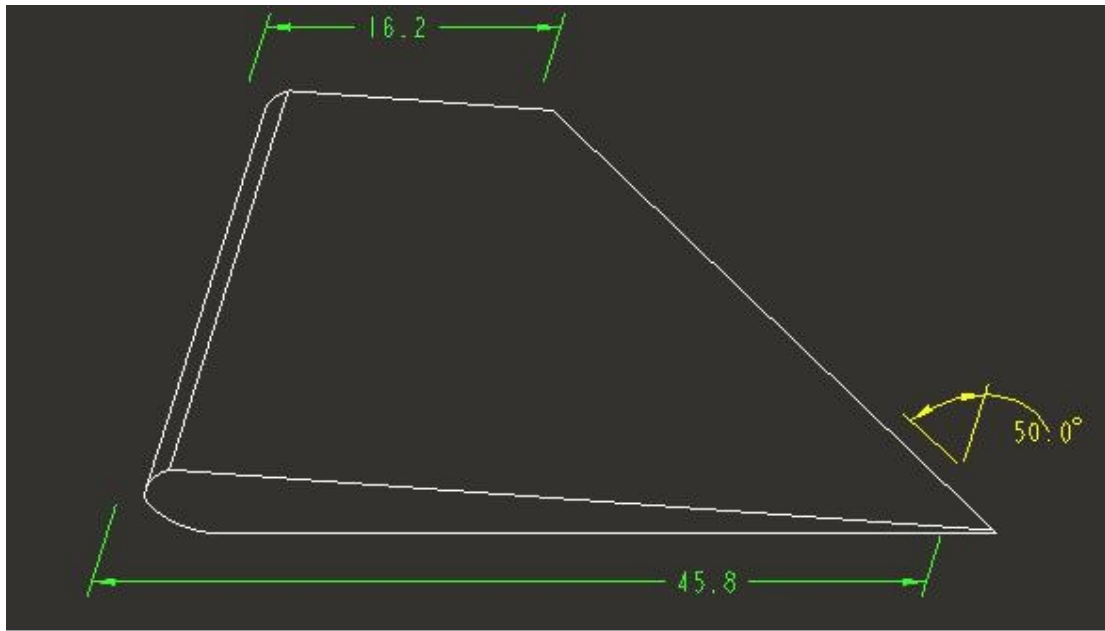

Figure 19. Geometry of a wing
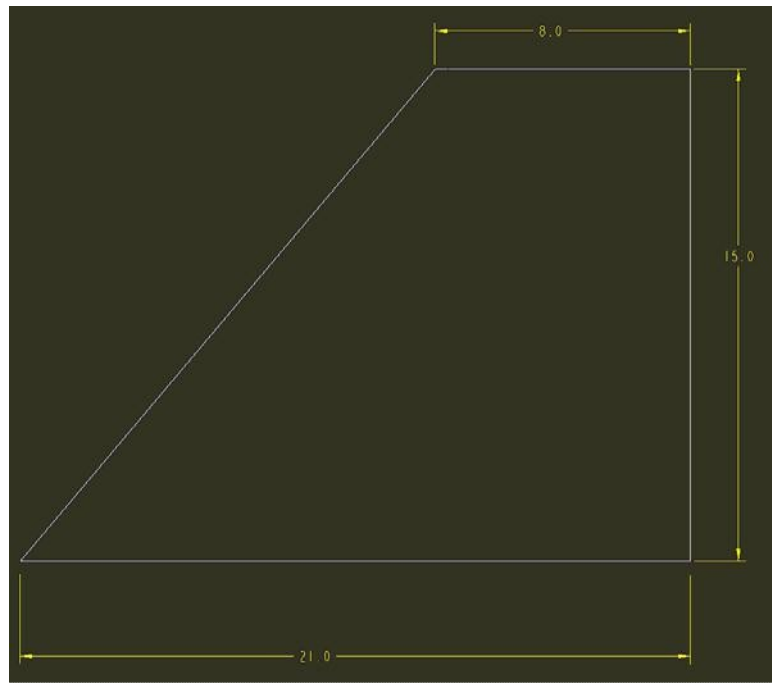
Figure 20. Geometry of a winglet

Table 8. Wing and lateral surface parameters

AR	3.45
Wing area	3175 ft^2
taper ratio	0.47
Re	2.31 x 10^7
Airfoil, root	Clark Y
Airfoil, tip	Clark Y
C_l	1.4
Aerodynamic Center (x, y)	(8 ft, 32 ft)
Twist angle, i_w	−1°
Dihedral angle, G	2°

LE sweep, L_{LE}	5°
TE sweep, L_{TE}	50°
Elevator, A_e	None
Aileron, A_a	None
Taper Ratio, $l = c_t/c_r$	0.47
Spoilers	no
Flaps	no
Leading-edge Devices	no
Winglets	yes

Chapter 7. Empennage Design

The tilted vertical tail protects the tail wing from exposure to a downwash of the front wing compared to a T-tail configuration. The tilted vertical tail improves product of tail moment arm as well as the tail lift curve slope. Since the vertical tail interfere with the fuselage and the horizontal tail, its aspect ratio increases. The local dynamic pressure is reduced due to the converging fuselage flow going over the tail. The horizontal stabilizer helps pull the plane''s tail down to balance the wing C.G. moment. Though this type of configuration is easy and safe, it is not aerodynamically efficient since the engine has to use twice as much power to balance the plane.

By having T-tail, some aerodynamics advantages can be gained. Having mounted T-tail, the tailplane is kept out of airflow behind the wings. By having smooth flow over the tail, the better pitch control can be gained. T-tail is high mounted therefore; it can be out of way of rear fuselage and this configuration is beneficial for planes that have engines in the rear fuselage. Another advantage of having T-tail is the increased distance between wings and tail plane since it does not have significant effect on aircraft weight. But there are some other disadvantages of having T-tail. During deep stall, a stalled wing will block the flow over the tail plane, resulting in total loss of pitch control. To support the forces produced by the tail, the fin has to be made stiff and stronger which results in increasing aircraft weight. Since the elevator surfaces are distant from the ground, it makes difficult to check elevators from ground.

7.1. Design of the horizontal stabilizer

4
4

The volume method was utilized to find the surface area of the horizontal stabilizer. The distance between the wing and tail wing was 6 ft. The equation is as follows:

$$S_{HT} = \frac{V_h * C_A * }{L} \qquad (21)$$

Using a volume coefficient of 0.44 and the wing parameters, the area of the horizontal stabilizer was calculated to be 668 ft^2. The aspect ratio for the horizontal stabilizer was assumed to be 2.2 based on table 8.13 in reference [7]. Using this data, the root chord of the horizontal stabilizer was determined to be 15.9 ft and the tip chord was 9.1 ft.

The taper ratio was calculated to be 0.57 for the horizontal stabilizer. It will also have 10q of leading edge sweep.

The NACA 4412 was chosen as the airfoil design for the horizontal stabilizer. The maximum lift coefficient of the NACA 4412 airfoil is 1.65. This parameter is very important as the maximum lift of the wing is strongly connected to it and it is therefore decisive for the minimum airspeed at which an aircraft can still fly horizontally. It is also seen over the years that NACA 4412''s characteristics with standard roughness such as dust and bug deposits does not affect lift characteristics. It is a moderately cambered airfoil with a nearly flat bottom. Cambering an airfoil helps provide it with a higher maximum lift coefficient.
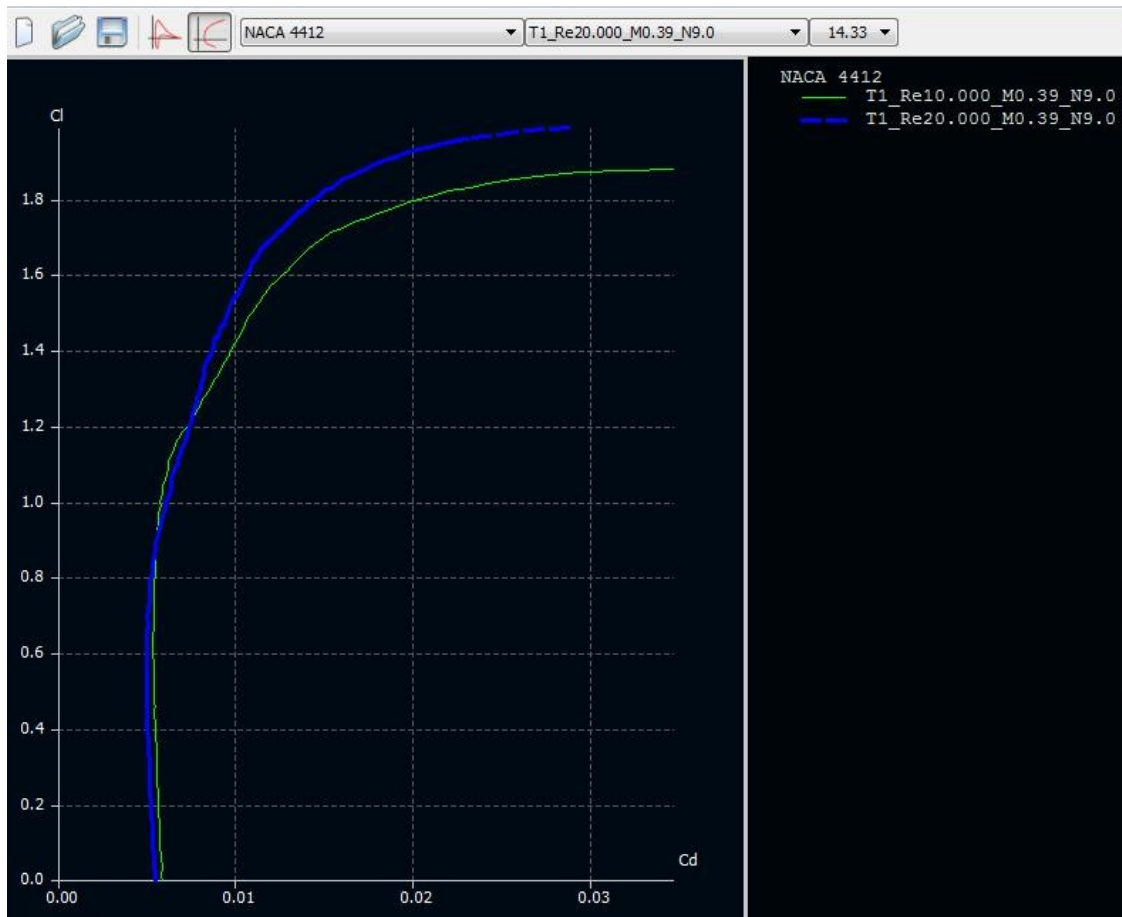
Figure 21. Shape of NACA 4412 airfoil

Figure 22. Lift coefficient vs Drag coefficient for NACA 4412 airfoil

The incidence angle of the horizontal stabilizer is assumed to be - 1q

as to produce a down force to counteract the lifting force of the main

wing on the airplane. Hoverwing''s

horizontal stabilizer will also have 10° of dihedral angle. It will have the taper ratio of 0.57.

7.2. Design of the vertical stabilizer

The area of the vertical stabilizer was found by the volume method with the following equation:

$$V_V \quad \frac{X_V S_V}{Sb} \tag{22}$$

Using a volume coefficient similar to flying boats of 0.032 and the wing parameters, a vertical tail area of 195 ft^2 is calculated. The aspect ratio of the vertical stabilizer was assumed to be 1.3 based on table 8.14 from reference [7]. Hoverwing will have two vertical stabilizers. The area calculated above is for one vertical stabilizer. The vertical stabilizer is recommended to be as small as possible to avoid height weathercock stability. If an airplane is yawed due to a gust of wind, its ability to automatically return to its previous heading depends on the area behind its center of gravity to produce a restoring force. The fuselage ahead of the center of gravity will tend to produce a force to destabilize the aircraft. This is called weathercock stability. Below formula is used to calculate vertical stabilizer area:

$$n_v = \frac{S_F l}{Sb} a \tag{23}$$ Based on the equation above, the area of the vertical tail was

calculated to be 169 ft^2, which is very close to that calculated using equations from reference [8]. The taper ratio of our vertical stabilizer is 0.58. The vertical stabilizer will have 50° leading edge sweep. The vertical stabilizer will have no dihedral angle and will be located 90° from the

horizontal tail. NACA 0012 airfoil will be used for the vertical stabilizer for simplicity

reasons. Figure 23 shows the lift coefficient curve for NACA 0012. This was calculated

using XFLR software.

Figure 23. Lift coefficient vs Drag coefficient for NACA 0012 airfoil
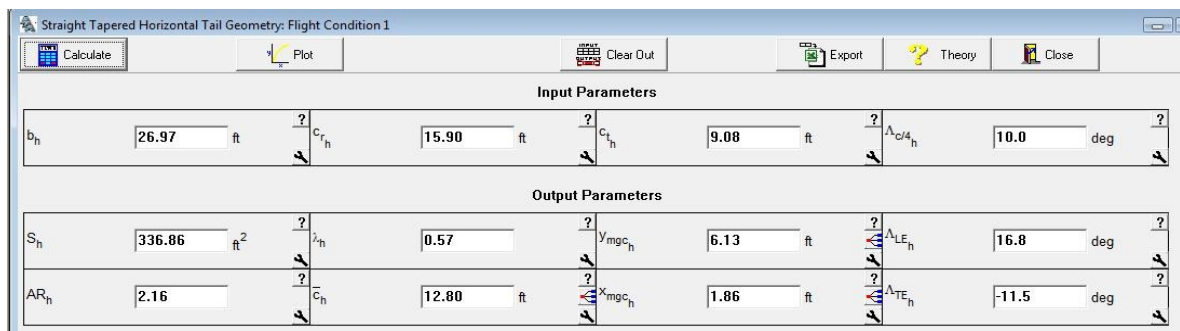
7.3. Empennage design evaluation

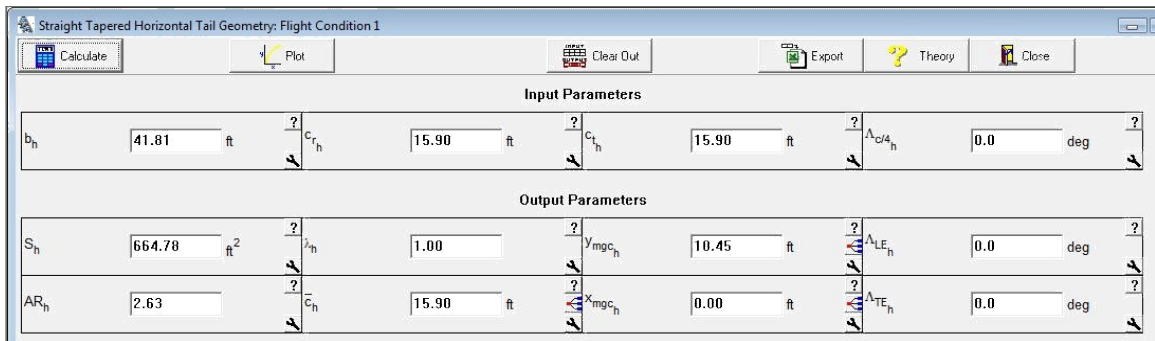Figure 24. Horizontal tail geometry tapered using AAA

Figure 25. Horizontal tail geometry untapered using AAA

As seen in above figures, part of the horizontal wing is untapered, therefore, two different

calculations were run in AAA, one for tapered part and other for the untapered part. The

reason for part of the horizontal tail is untapered is so that the installment of vertical tail

to horizontal tail is easier. The planform of the horizontal tail was incorrect in AAA,
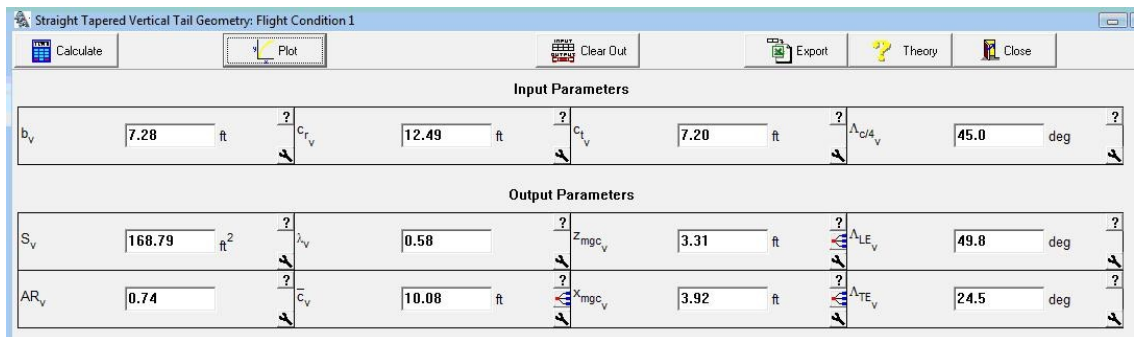
therefore it is not included.

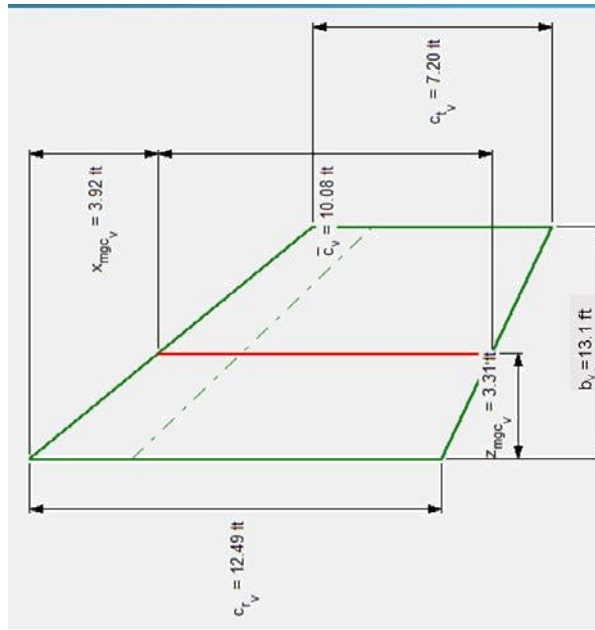Figure 26. Vertical tail geometry using AAA

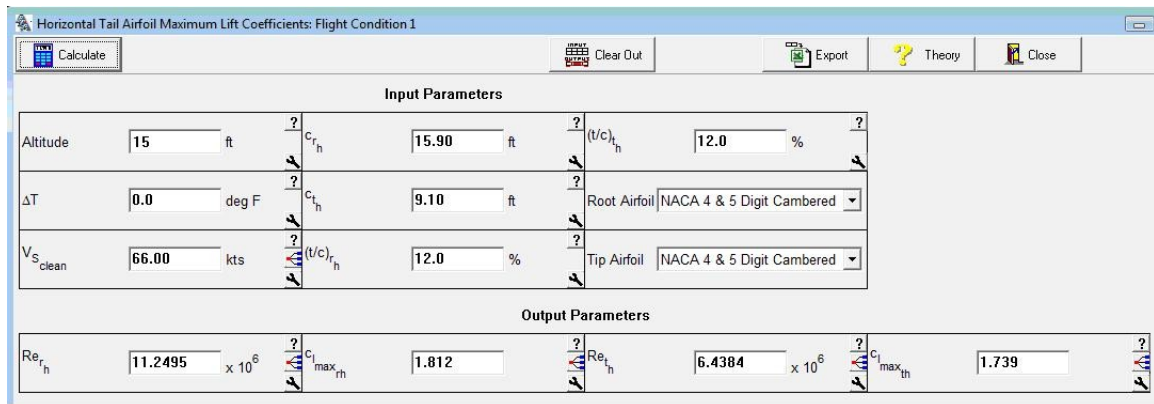Figure 27. Vertical tail planform using AAA

Figure 28. Lift coefficient for horizontal tail of the hoverwing

When the values were entered into AAA program, the Reynolds number came out to be

about in 10^6 range. Even though the same airfoil is being used for horizontal and

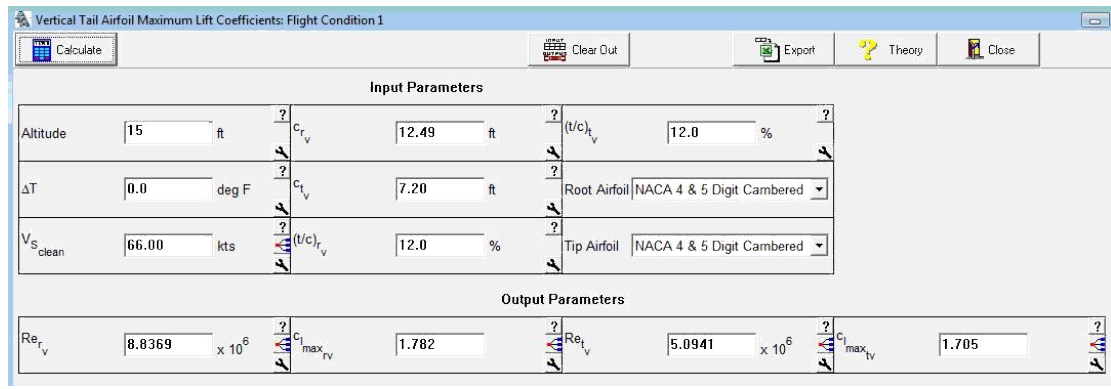vertical tails, Reynolds number came out to be different for both tails.

Figure 29. Lift coefficient for vertical tail of the hoverwing

7.4. Design of the longitudinal and directional controls

The vertical tail will have a rudder and the horizontal tail will have an elevator. The rudder surface area will be 30% of the vertical tail area. This will provide enough force for directional control and maneuvering. Since Hoverwing is designed to mostly fly in straight path, the rudder and elevator will not need to be larger as they will only be used for small directional change. The elevator will be 35% of the horizontal stabilizer area [8]. This will provide an effective elevator authority to control the aircraft and provide longitudinal stability.

7.5. CAD drawings

Figure 30 and 31 shows the geometry of the vertical tail and its control surfaces and figure 32 and 33 shows the horizontal tail and its control surfaces.
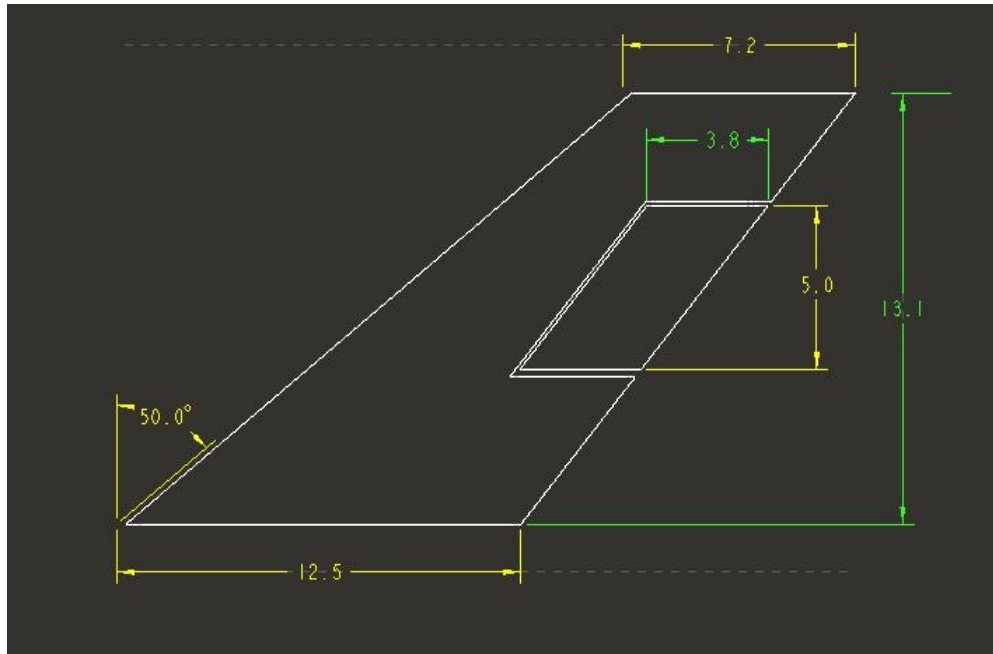
Figure 30. Geometry of a vertical stabilizer
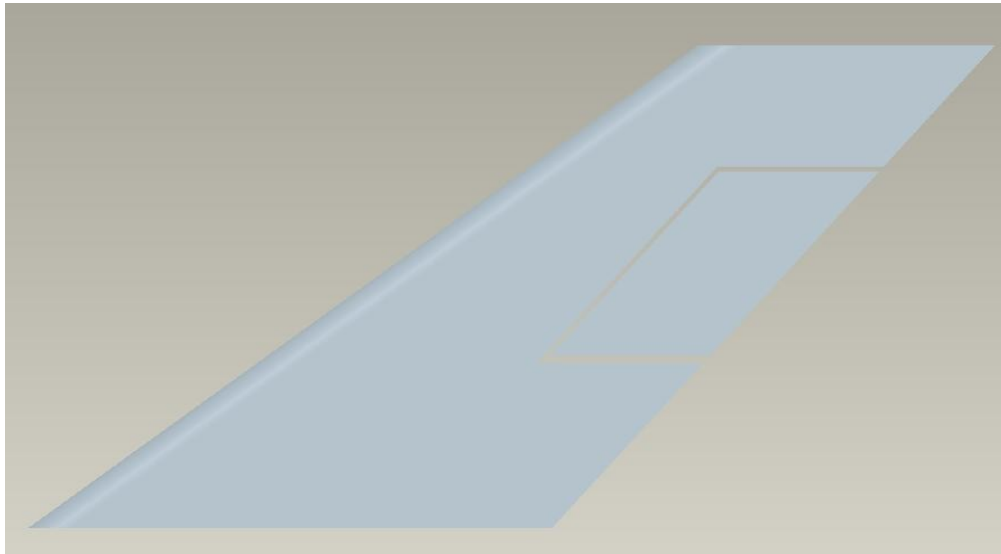
Figure 31. 3D picture of a vertical stabilizer
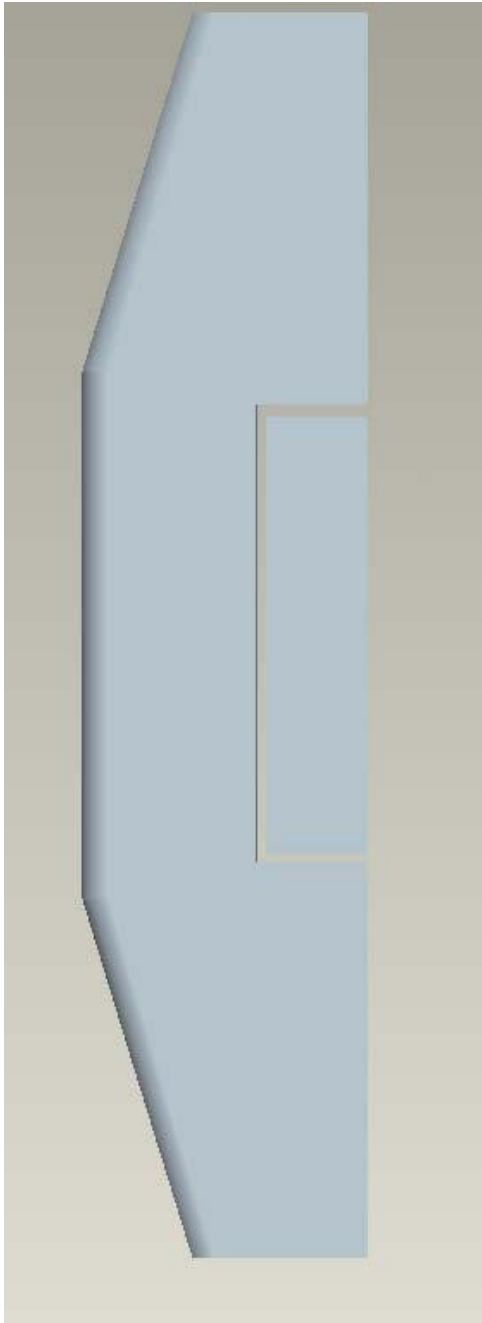
Figure 32. 3D picture of a horizontal stabilizer
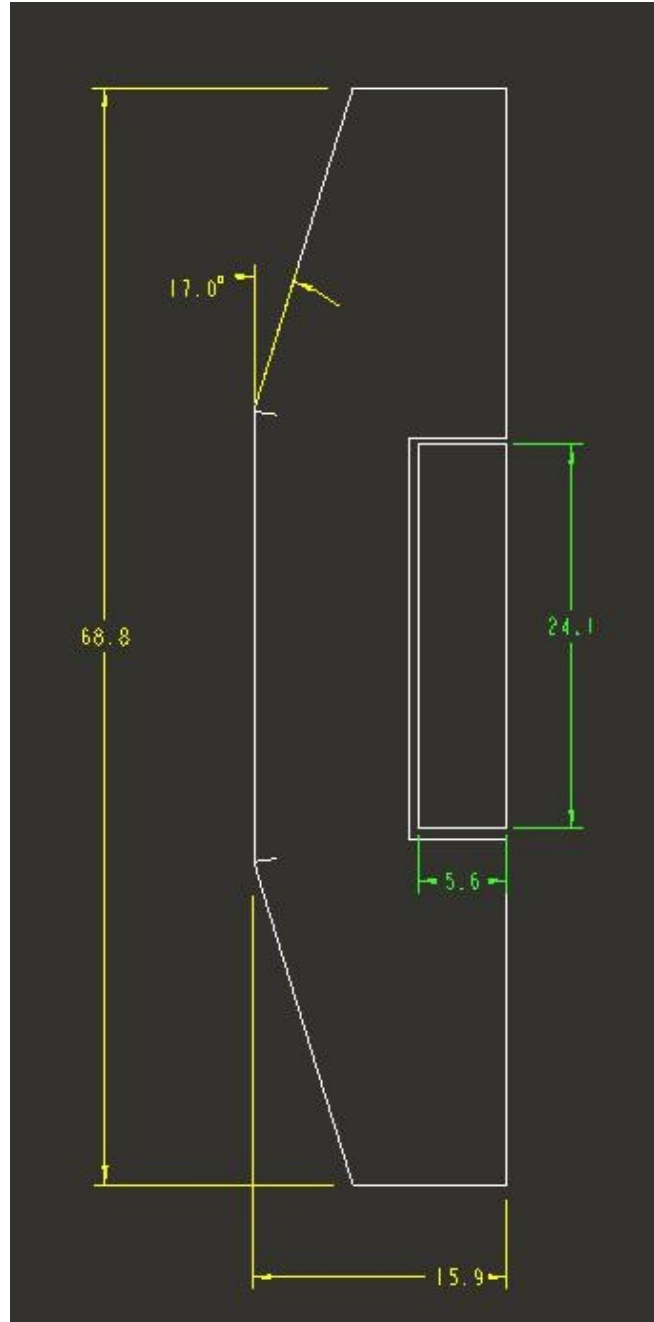
Figure 33. Geometry of a horizontal stabilizer

Table 9. Horizontal and vertical tail parameters

	Horizontal Tail	Vertical Tail
Airfoil	NACA 4412	NACA 0012
C_{LMAX}	1.5	1.3
Dihedral angle	10°	None
Taper Ratio	0.57	0.58
Aspect Ratio	2.2	1.3
Sweep angle	10°	50°
Incidence Angle	-1°	None
Control Surfaces	Elevator	Rudder
Sizes of Control Surfaces	24.10 ft x 5.6 ft	5.0 ft x 3.8 ft

Chapter 8. Weight and Balance Analysis

8.1. Component weight breakdown

The estimation of centre of gravity location for the airplane is calculated based on weight break down of major components of airplane. From weight sizing calculations we have,

x Gross Take off Weight, W_{TO} = 66,333 lbs

x Empty Weight, W_E = 41,033 lbs

x Mission Fuel Weight, W_F = 8,286 lbs

x Payload Weight = 16,820 lbs

x Crew Weight, W_{crew} = 375 lbs

Hoverwing is a water based aircraft which flies in ground effect. The Class I weight estimation was not helpful since reference [9] did not have published data on flying boats. The Class II Method for weight estimation of the components was used.

8.1.1. Wing group weight

The wing weight fraction, W_w / W_{zf}, depends upon the design limit normal maneuvering load factor through $n_{ult} = 1.5 n_{limit}$. Reference [8] offers the following equation for initially estimating the weight of the wing group

$$W_w \quad 0.0017 W_{MZF} \left(\frac{b}{\cos \Lambda_{1/2}} \right)^{0.75} \left[1 \quad \left(\frac{6.3 \cos \Lambda_{1/2}}{b} \right)^{1/2} \right] (n_{ult})^{0.55} \left(\frac{bS}{W_{MZF} \cos \Lambda_{1/2}} \right)^{0.30} \quad (24)$$

This equation is written for lengths in feet and weights in pounds; the quantities W_{zf} and

$t_{r,max}$ denote aircraft zero-fuel weight and wing root maximum thickness, respectively.

8.1.2. Fuselage group weight

For Hoverwing, the flying boat equation is used to calculate the fuselage weight.

$$W_{f,fl.boat} = 1.65W_f \qquad\qquad (25)$$

It is surprising that the design normal load factor does not appear in the fuselage weight equation. It is suggested that pressure forces acting on the fuselage shell are more significant than the fore and aft bending moments acting at the wing-fuselage juncture. The fuselage weight is difficult to estimate because it is a complex structure with many openings, support attachments, floors, etc., but it is strongly dependent on the gross shell area, S_g. This is the surface area of the complete fuselage treated as an ideal surface, that is, with no cutouts for windows or wing and tail attachments. Methods for approximating the gross shell area are given in Appendix B in reference [8]. The fuselage weight may then be approximated by

$$W_f \quad 0.02 K_f \left\{ \frac{V_D \, l_h}{W_f \quad h_f} \right\}^{1/2} (S_{fgs})^{1.2} \qquad\qquad (26)$$

In this equation the lengths are in feet, the weight is in pounds, and the design dive speed, V_D, is in knots. The length l_h is the distance between the root quarter-chord points of the tail and the wing. Above equation was also used to calculate boom weight where W_f and h_f was replaced by W_b and h_b. To this basic weight, 7% should be added if the engines are mounted on the aft fuselage.

8.1.3. Tail group weight

This group also represents a small fraction of the take-off weight, about 2% to 3%, but that weight does have an effect on center of gravity location because of the long moment arms. Reference [8] suggests the following functional relationships:

$$\frac{W_.}{k_h S_h} \quad f \cdot \left(\S \frac{S_k^{0.2} V_{D,E}}{\sqrt{\cos l_h}} \right)_i$$

(27)

$$\frac{W_.}{k_v S_v} \quad g \cdot \left(\S \frac{S_v^{0.2} V_{D,E}}{\sqrt{\cos l_v}} \right)_i$$

(28)

The coefficients k_h and k_v account for different tail configurations. For example, current practice for airliners is to have variable incidence tails, and k_h=1.1, while a fixed horizontal stabilizer would have k_h=1.0, reflecting the lighter structure typical of fixed equipment. For fuselage-mounted vertical tails k_v=1.0 while for T-tails $k_v \quad 1 \quad 0.15 \frac{S_h h_h}{S_v b_v}$.

In this last equation the quantities h_h and b_v correspond to the height of the horizontal tail above the fuselage centerline and the height of the tip of the vertical tail above the fuselage centerline, respectively.

$$W_h \quad K_h S_h [3.81 \frac{S_h^{0.2} V_D}{(1000 \cos 9_{1/2_h})^{1/2}} \quad 0.287]$$

(29)

$$W_v \quad K_v S_v [3.81 \cdot \frac{S_v^{0.2} V_D}{(1000 \cos 9_{1/2_h})^{1/2}} \quad 0.287]$$

(30)

The weight calculations of the power plant group and fixed equipment group weight equations were obtained using below equations [11].

Commercial Transport Airplanes Engine Weight Estimation:

$W_e = N_e W_{eng}''$ (31)

Air Induction System Weight Estimation General Aviation Airplanes Torenbeek Method:
$W_{ai}+W_p =$
$1.03(N_e)^{0.3}(P_{TO})^{0.7}$ (32)

Propeller Weight Estimation Commercial Transport Airplanes Torenbeek Method:

$$W_{prop} = K_{prop2}(N_p)^{0.218}\{D_P P_{TO}(N_{Bl})^{1/2}\}^{0.782} \tag{33}$$

Fuel System Weight Estimation Commercial Transport Airplanes GD Method:

For a fuel system with self-sealing bladder cells:

$$W_{fs} = 41.6\{(W_F/K_{fps})/100\}^{0.818}+W_{supp} \tag{34}$$

Propulsion System Weight Estimation Commercial Transport Airplanes GD Method

Engine Controls for fuselage mounted engines

$$W_{ec} = K_{ec}(l_f N_e)^{0.792} \tag{35}$$

Propulsion System Weight Estimation Commercial Transport Airplanes GD Method

Engine starting system for airplanes with turboprop engines using pneumatic starting systems:

$$W_{ess} = 12.05(W_e/1,000)^{1.458} \tag{36}$$

Propulsion System Weight Estimation Commercial Transport Airplanes GD Method

Propeller Controls for turboprop engines:

$$W_{pc} = 0.322(N_{bl})^{0.589}\{(N_p D_p P_{TO}/N_e)/1,000\}^{1.178} \tag{37}$$

Flight Control System Weight Estimation Commercial Transport Airplanes Torenbeek Method:

$$W_{fc} = K_{fc}(W_{TO})^{2/3} \tag{38}$$

Hydraulic and/or Pneumatic System Weight Estimation for commercial transports:

0.0060-0.0120 of W_{TO}

Hydraulic and/or Pneumatic System Weight Estimation Commercial Transport Airplanes

Torenbeek Method for propeller driven transports:

$$W_{hps}+W_{els} = 0.325(W_E)^{0.8} \tag{39}$$

Weight Estimation For The Oxygen System Commercial Transport Airplanes Torenbeek Method for flights below 25,000 ft:

$$W_{ox} = 20+0.5N_{pax} \tag{40}$$

Auxiliary Power Unit Weight Estimation

$$W_{apu} = (0.004 \text{ to } 0.013)W_{TO} \tag{41}$$

Furnishings Weight Estimation General Aviation Airplanes Torenbeek Method for single engine airplanes:

$$W_{fur} = 5+13N_{pax}+25N_{row} \tag{42}$$

Weight Estimation For Auxiliary Gear:

$$W_{aux} = 0.01W_E \tag{43}$$

Estimating Weight of Paint

$$W_{pt} = 0.003W_{TO} \text{ to } 0.006W_{TO} \tag{44}$$

Table 10. Determination of preliminary component weight of the hoverwing

Major Comp.	Sub-categories	W, lbs
Structure Weight, Wstruct	Wing	4410
Empennage	H. Tail	962.00
2 Vertical Tails	V. Tail (each)	245.00
2 Booms	Boom (each)	4773.00
	Nacelles	689.00
	Fuselage	8393.00
Power Plant Weight, Wpr	Engine	2025.00

	Propeller	1263.00
	Fuel System	438.00
	Propulsion	5719.00
	Control	200.00
Fixed Equipm. Weight, Wfeq	Avioni+Instru	150
	Surface Controls	1098
	Hydraulic System	654
	Electrical System	1643
	Electronics	192
	APU	464
	Furnishing	200
	Auxiliary Gear	460
	Baggage & Cargo	262
	Paint	460

Table 10 defines the determination of the component weight break down for the proposed design. When the numbers in the first column are added, they yield an empty weight of 39,718 lbs instead of the desired weight of 41,033 lbs. The error is around 0.05% therefore the results are acceptable. We have to keep in mind that Hoverwing is a bridge between ship and airplane therefore the equation used to calculate the weight of the components are not completely accurate, due to this factor the error margin is calculated. If the judgment is made to manufacture the proposed design with composites as primary

structural materials, significant weight savings can be obtained. A reasonable assumption is to apply a 10% weight reduction to wing, empennage, fuselage and nacelles.
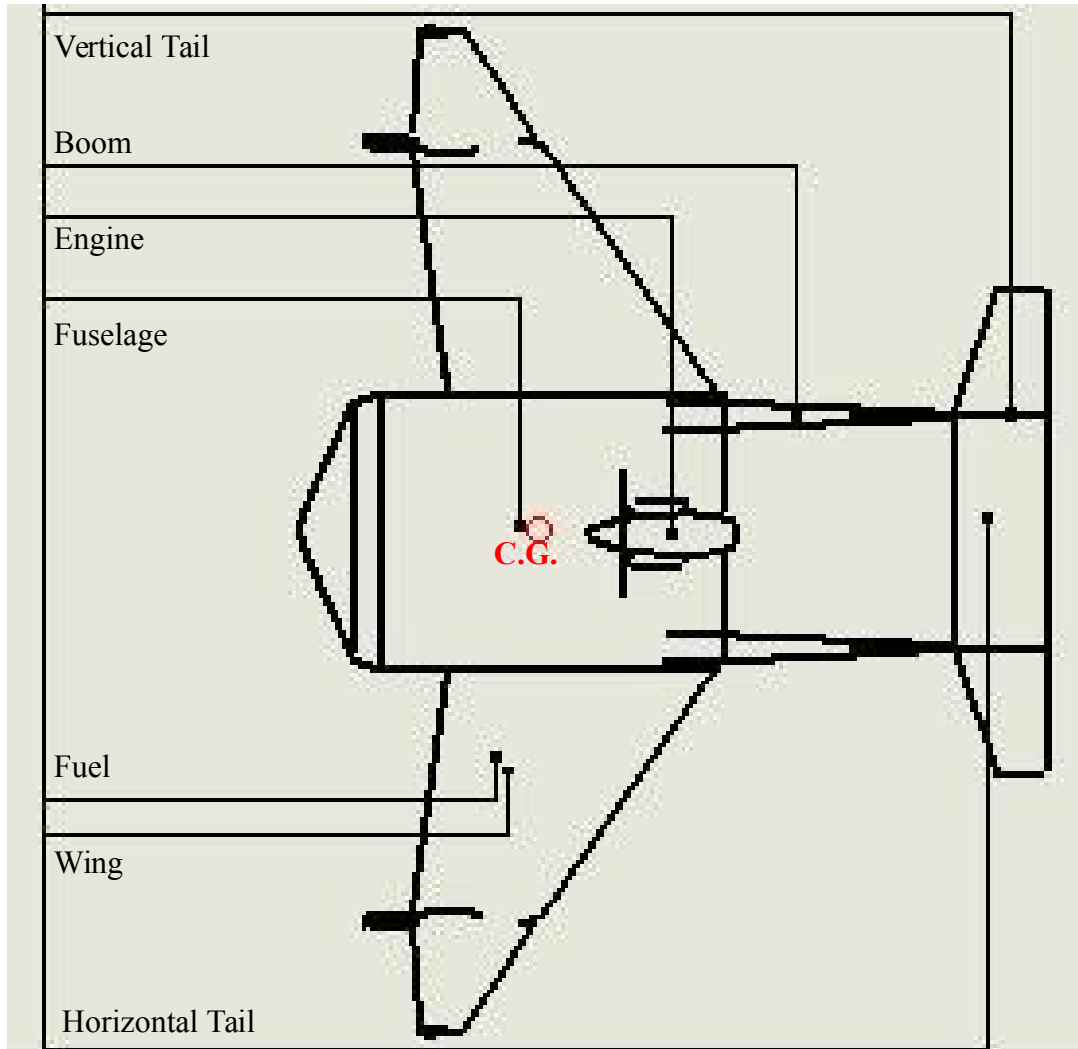

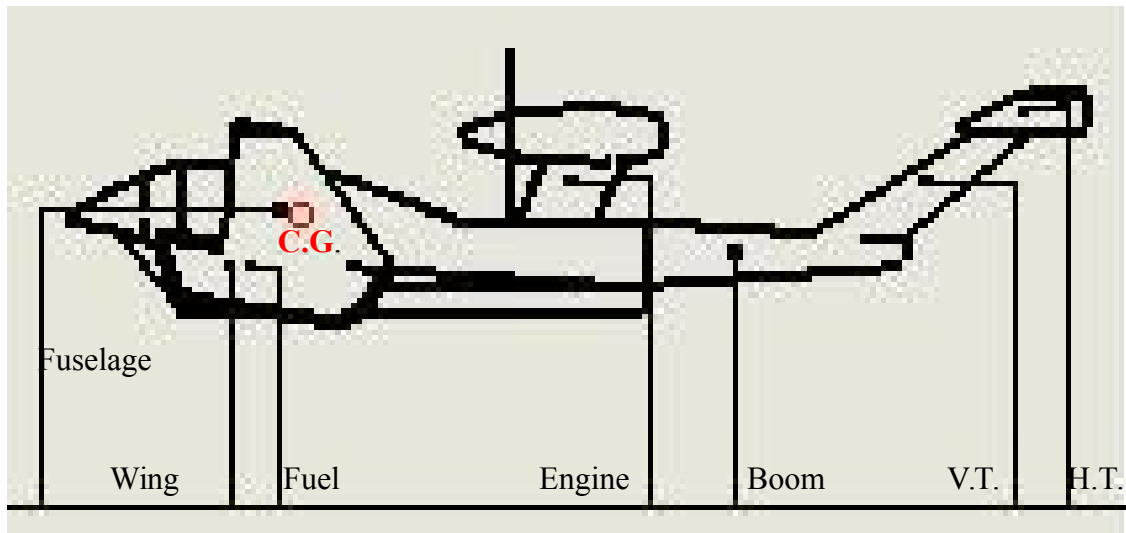Figure 34. Location of centre of gravity in X-direction

Figure 35. Location of centre of gravity in Y-direction

Figure 34 and Figure 35 represents the Centre of gravity locations of major components for the proposed design in X and Z directions. The X, Y, Z coordinates of each component centre of gravity are tabulated in Table 11. The zero reference point is considered so that all the coordinates are positive. Table 11. Component weight and coordinate data

Major Comp.	Component	W	xi	xi + 10	Wixi	yi	yi + 10	Wiyi	zi	zi + 10	Wizi
Structure Weight, Wstruct	Wing	4410	433.08	434.08	1914292.8	726	736	3245760	0	0	0
	H. Tail	962	1223.28	1233.3	1161749.76	1256	1266	1192572	0	0	0
	V. Tail	245	1199.28	1209.3	272088	1246	1256	282600	0	0	0
	Boom	4773	923.28	933.28	4407881.44	650	660	3117180	0	0	0
	Nacelles	689	660	670	448230	588	598	400062	0	0	0
	Fuselage	8393	388.48	398.48	3322492.89	204	214	1784332	0	0	0
	Power Plant Installation	9645	170	180	1724760	372	382	3660324	0	0	0
	Fixed Equipment	5583	198	208	1099072	680	690	3645960	0	0	0
	Fuel	8286	433.44	443.44	3674343.84	180	190	1574340	0	0	0
	Payload	16820	540	550	9251000	168	178	2993960	0	0	0
	WTO	**66300**	**xcg total:**	388.21	27275910.7	**ycg total:**	261.4	21897090	**zcg Tot.:**	0	0

62

The centre of gravity locations must be calculated for all feasible loading scenarios. The loading scenarios depend to a large extent on the mission of the airplane. Typical loading combinations are,

1. Empty Weight

2. Empty Weight + Fuel

3. Empty Weight + Payload + Fuel

4. Empty Weight + Crew + Fuel + Payload = Take off Weight

5. Empty Weight + Crew + Payload

As mentioned in Figure 28 and Figure 29, the centre of gravity for these loading scenarios is calculated.

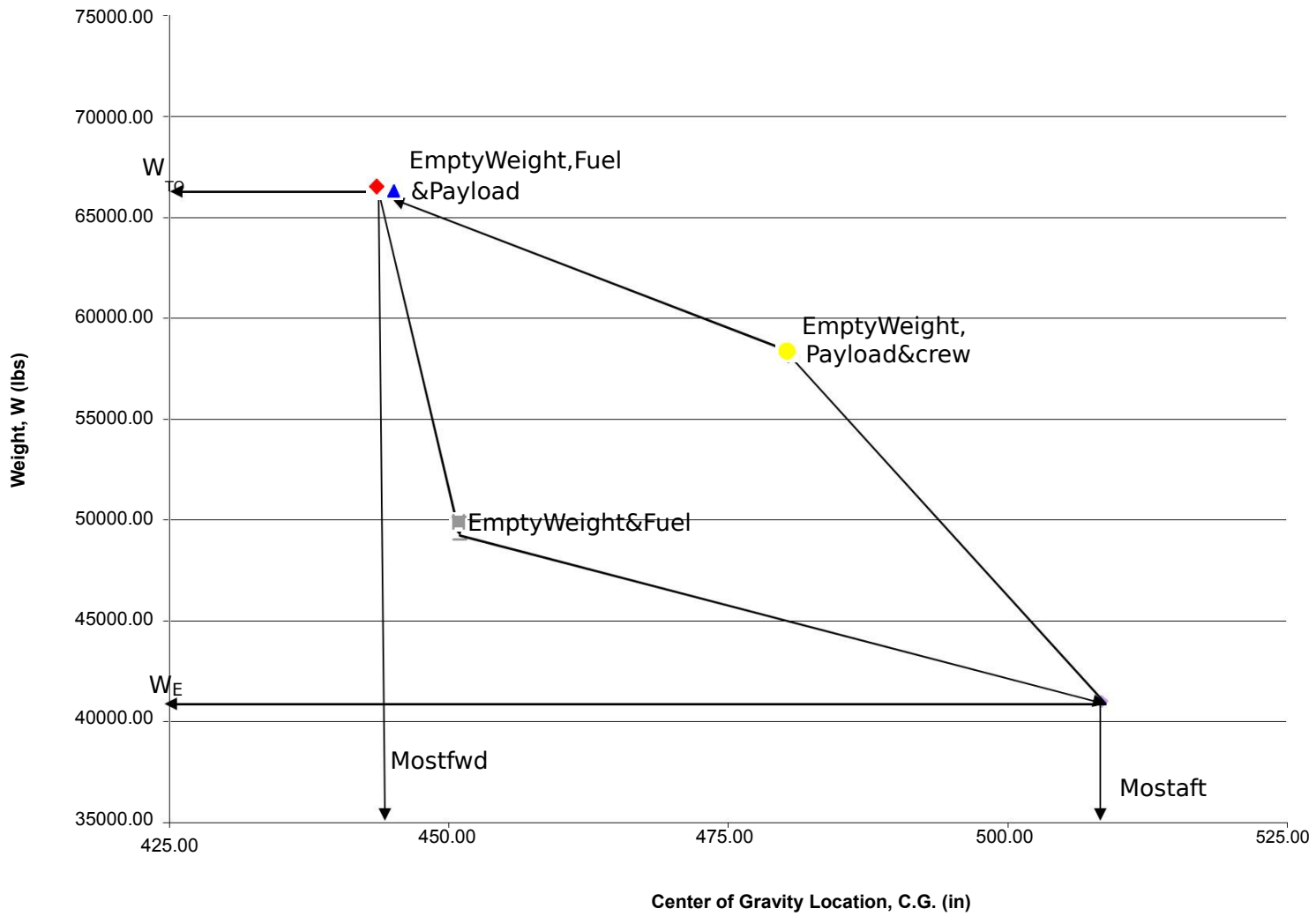| 1.	Weight Empty	41000	508.37
2.	Empty Weight+Fuel	49826	450.98
3.	Empty Weight+Payload+Fuel	66106	445.11
4.	Takeoff Weight	66300	443.60
5.	Empty Weight+Crew+Payload	58195	480.33

Figure 36. Center of Gravity excursion diagram

Figure 30 represents the C.G excursion diagram of the proposed design. The loading sequences as well as the critical weights such as W_E and W_{TO} are determined. The C.G locations are plotted in terms of fuselage station (F.S). From Figure 68, the most forward C.G occurs at $W = 66300$ lbs, F.S $= 443.60$ in. and most aft C.G occurs at $W = 41000$ lbs, F.S $= 508.37$ in.

The parametric study is performed based on the proposed mission specification by using wing analysis program. The sweep angle for the proposed wing design is 50^n, so here I performed the study for 48^n, 50^n and 52^n for a fixed aspect ratio and varying the taper ratio from 0.4 to 0.6 and twist from -5^n to $+5^n$. The results from parametric study matched to that of matching graph as discussed in section 3.6

Chapter 9. Stability and control analysis

9.1. Static longitudinal stability

Figure 31 represents the longitudinal X-plot. Note that the two legs of the X

are representative of,

1. The c.g leg represents the rate at which the c.g moves aft(fwd) as a function of

    horizontal tail area.

2. The a.c leg represents the rate at which the a.c moves aft (fwd) as a function of
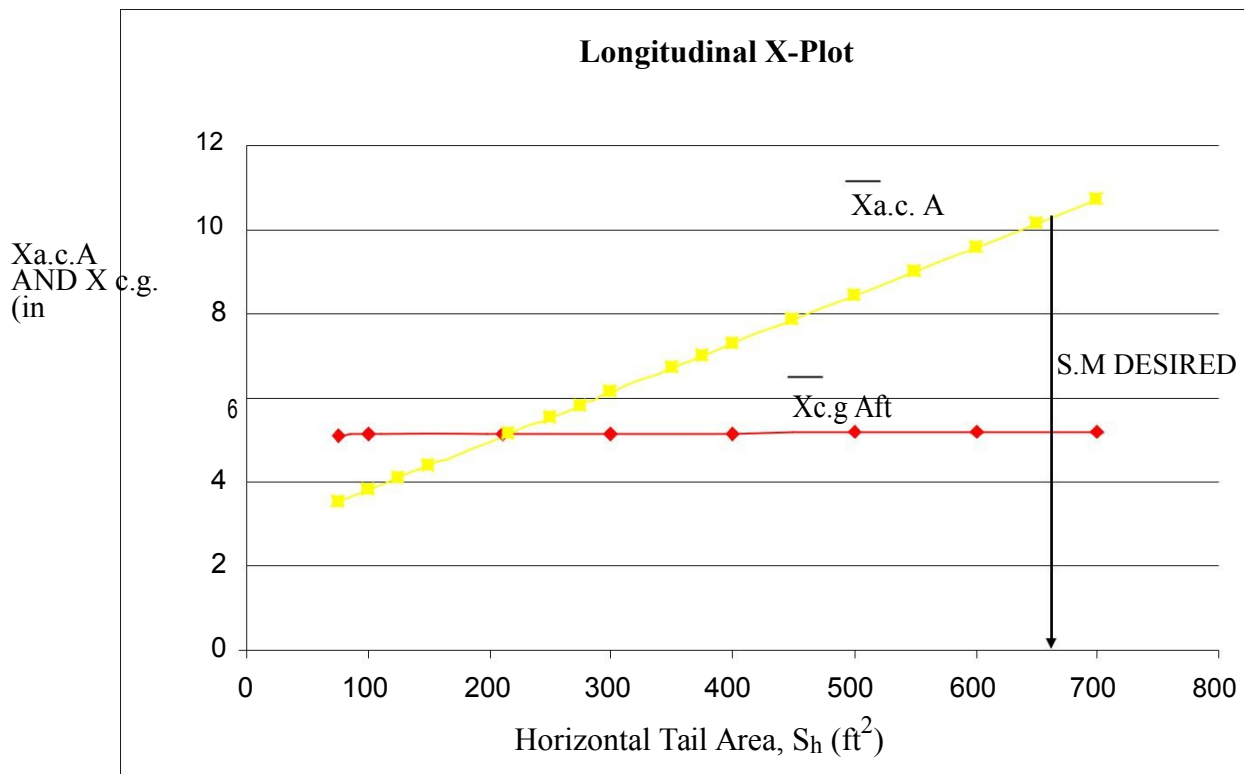
    horizontal tail area [11].

Figure 37. Longitudinal X-plot

The c.g leg is calculated with the help of the class II weight and balance analysis. From the

class II weight analysis the weight of the horizontal tail is known on a per ft^2 basis.

Assuming this quantity to be independent of surface area, the c.g can be found for any area of the horizontal tail.

The a.c leg is calculated with the following equations:

$$\overline{X}_{ac_A} \quad \frac{[\overline{X}_{ac_{wb}} \quad \frac{\{C_{L_D}(1 \quad \frac{dH_h}{}) (\frac{S_h}{})\overline{X}_{ac_h} \quad \frac{C_{L_D}}{}_c (1 \quad \frac{dH_c}{dD})\overline{X}_{ac_c}(\frac{S_c}{})\}}{C_{L_D}{}_{wb}}]}{F} \quad (45)$$

Where

$$F \quad [1\{ \quad \frac{\{C_{L_D} (1 \quad \frac{dH_h}{}_h)(\frac{S_h}{})\overline{X}^{ac}{}_h \quad \frac{C_{L_D}}{}_c (1 \quad \frac{dH_c}{})\overline{X}_{ac_c}(\frac{S_c}{})\}}{C_{L_{Dwb}}} \quad (46)$$

The aerodynamic quantities can be computed with methods presented in reference [8]. As the proposed design is a tail-aft airplane, therefore set $S_c = 0$ and consider S_h as the independent variable. Both the c.g and the a.c leg of the ''X'' can now are plotted as a function of area. This completes the longitudinal X-plot. The wing lift curve slope may be estimated from the following equation.

$$C_{L_{Dw}} \quad [2 \quad \frac{2SA}{}$$

$$\{ \qquad A^2 \ E^{\ 2}$$

$$4\}^{1/2} \,] \quad \frac{\overline{}}{k^2\left(^1\right.} \tag{47}$$

$$\frac{\tan^2 \Lambda_{c/2})}{E_2}$$

Where: $A = \frac{b^2}{S}$ is the wing aspect ratio

$$E = \sqrt{(1 - M^2)} \tag{48}$$

$$k \frac{(C_{l_D})}{\sqrt{M^2})}(1-$$

(49)

$à_{c/2}$ is the semi chord sweep angle.

From wing calculations, we have

A =3.45 $à_{c/2} = 12°$

M = 0.12 $à_{c/4} = 18°$

By substituting the values in above equation, we get

$C_{L_{lW}}$ = 3.68 rad^{-1}

The airplane lift cure slope may be estimated from,

$$C_{L_D} \quad C_{L_{D_{wf}}} \quad C_{L_{D_h}} K_h (\frac{S_h}{S})(1 \frac{dH}{dD}) \quad C_{L_{D_c}} K_c (\frac{S_c}{S})(1 \frac{dH_c}{dD})$$

(50)

Where:

$C_{L_{lwf}}$ is the wing fuselage (wing body) lift curve slope, given by

$$C_{L_D{}_{wf}} \quad K_{wf} C_{L_D{}_w}$$

(51)

Where: K_{wf} is the wing fuselage interference factor given by:

$$K_{wf} \quad 1 \quad 0.025(\frac{d_f}{b}) \quad 0.25(\frac{d_f}{b})^2$$

(52)

By performing the calculations and substituting the values in wing fuselage lift curve slope, we get

$C_{L_{lwf}}$ = 3.53 rad^{-1}

$\frac{dH}{dD}$ = down wash gradient at the horizontal tail which is equal to,

$$\frac{dH}{dD} \quad 4.44[\{\frac{K_A K_0 K_h \ (\cos'_{c/4}) \ 1}{2}\}^{1.19} \ ]\{\frac{(C_{L_D})_{atM}}{(C_{L_D})_{atM \ 0}}\} \tag{53}$$

Where,

$$K_A \quad (\frac{1}{A}) \quad \frac{1}{(1 \ A^{1.7})} \tag{54}$$

$$K_0 \quad \frac{(10 \ 3O)}{7} \tag{55}$$

$$K_h \quad \frac{(1 \ \frac{h}{b})}{(\frac{2l_h}{b})^{1/3}} \tag{56}$$
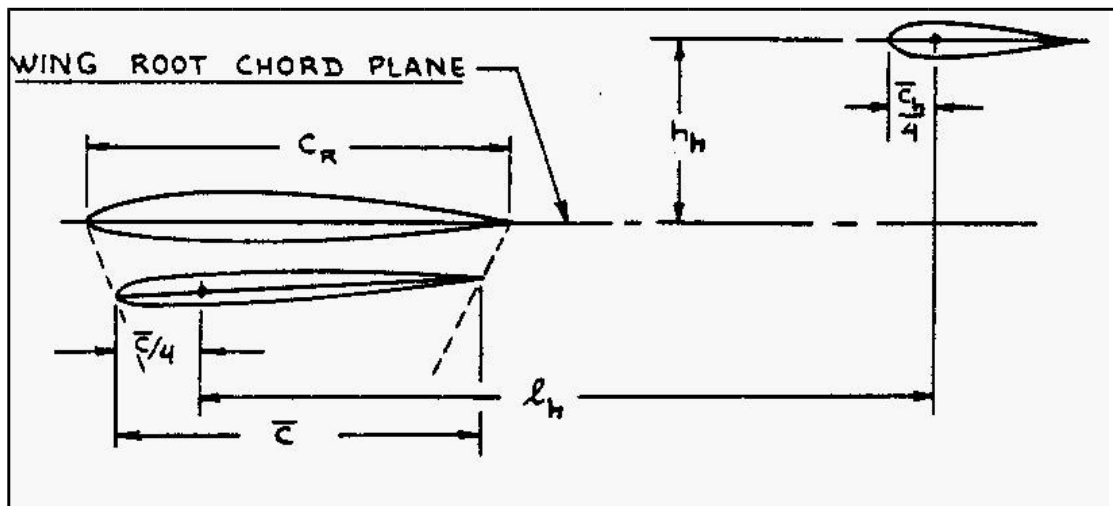

Figure 38. Geometric parameters for horizontal tail location

Based on Figure 38, the parameters for the l_h and h_h are calculated for the proposed design.

By substituting the values in above equation, we

get dİ/dİ = 0.505

The horizontal tail lift curve slope may be estimated from below equation.

$$C_{L_{D_s}} \quad \frac{2SA}{[2 \ \{\frac{\frac{A E}{22}}{k^2 (\frac{1 \ \tan^2 / _{c/2}}{E^2})} \quad 4\}^{1/2}]} \tag{57}$$

By substituting the values in above equation, we get

CLİh= 3.19 rad^{-1}

CLİ= 3.92 rad^{-1}

The following equation may be used to compute the location of the airplane aerodynamic

center in fractions of mean geometric chord.

$$\overline{X}_{ac_A} \quad \frac{[(X_{ac_{wf}})C_{L_{D_{wf}}} \quad \{K_h C_{L_{D_h}} (1 \frac{d\overline{H}}{dD})(\frac{S_h}{S})\overline{X}_{ac_h} \ K_c \ C_{L_{D_c}} (1 \frac{d\overline{H}}{dD})(\frac{S_c}{S})\overline{X}_{ac_c}\}]}{C_{L_D}} \tag{58}$$

Where:

$$\overline{X}^{ac}_{wf} \quad \overline{X}_{ac_w} \ ' \ \overline{X}_{ac_f} \tag{59}$$

$$' \overline{X}_{ac_f} \quad \frac{(\frac{dM}{dD})}{(\overline{q}S\overline{c}C_{L_D})} \tag{60}$$

$$(\frac{dM}{dD}) \ '(\frac{\overline{C}_{L_{D_w}}}{36.5})(\frac{}{0.08})[\sum_{i \ 1}^{i \ 13}\{(W_{f_i}) (\frac{2}{d})_i \ ' X_i \}] \tag{61}$$
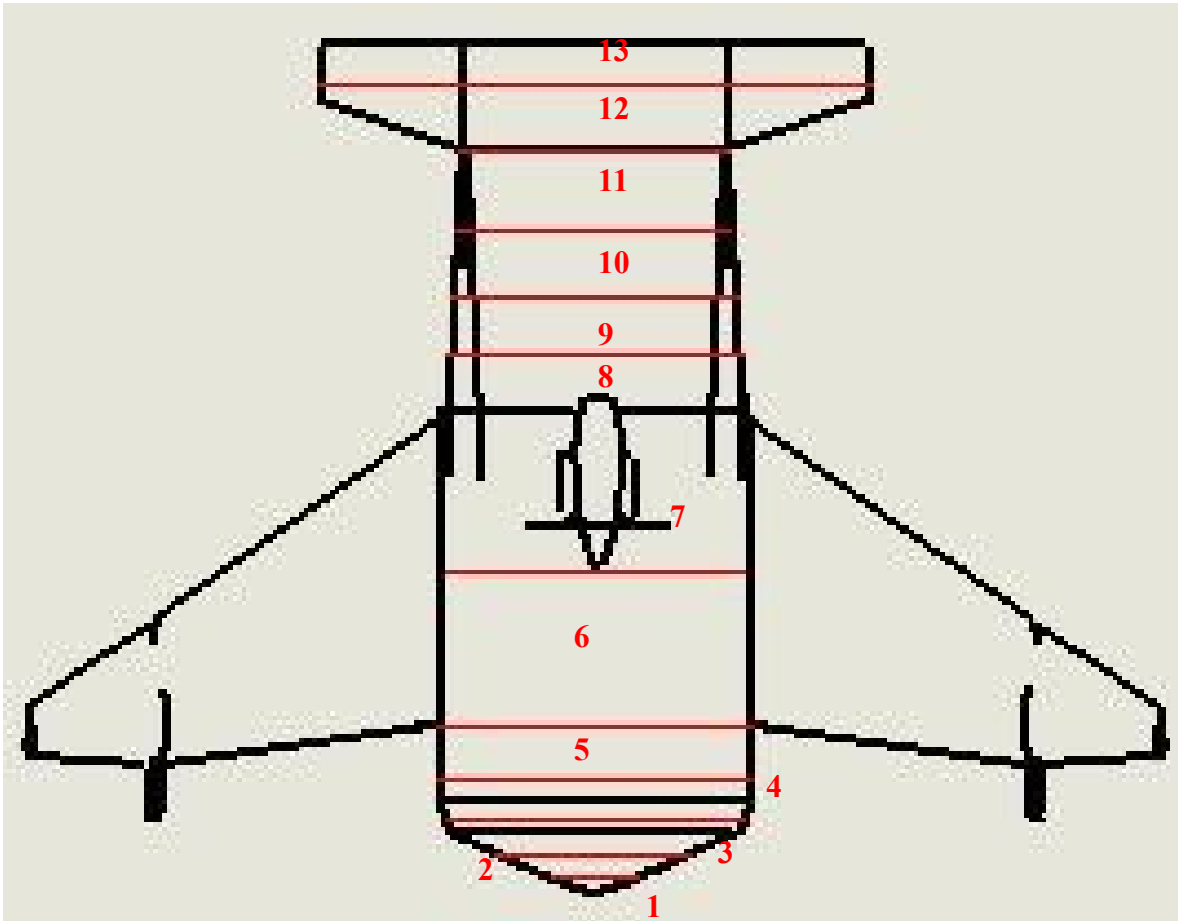
Figure 39. Layout for computing fuselage and contribution to airplane
aerodynamic center location

Table 12. Calculation of downwash gradient

I	W_f	$\ddot{X}_i$	$d\bar{H}/d\iota$
1	3.2	0.978	5.7
2	4.2	1.9	8.3
3	5.6	1.2	8.3
4	6.2	0.956	7.5
5	10.2	1.1	5.6
6	28.6	1.5	12.0

7	24.5	1.3	8.8
8	4.9	1.1	8.1
9	4.8	1.1	8.0
10	4.8	1.3	10.6
11	4.8	1.12	10.6
12	5.0	1.15	7.10
13	5.0	0.560	7.9

By substituting the values in downwash gradient equation, we

get $(dM/d\mathfrak{l}) = 9.6 * 10^6$

By substituting these values in equation, we get

$\overline{X}_{acA} = 5.154$

9.2. Static directional stability

Figure 38 shows the X-plot for static directional stability. The c.g leg is determined with

the help of class II weight analysis. The weight per ft^2 of the vertical tail is known from
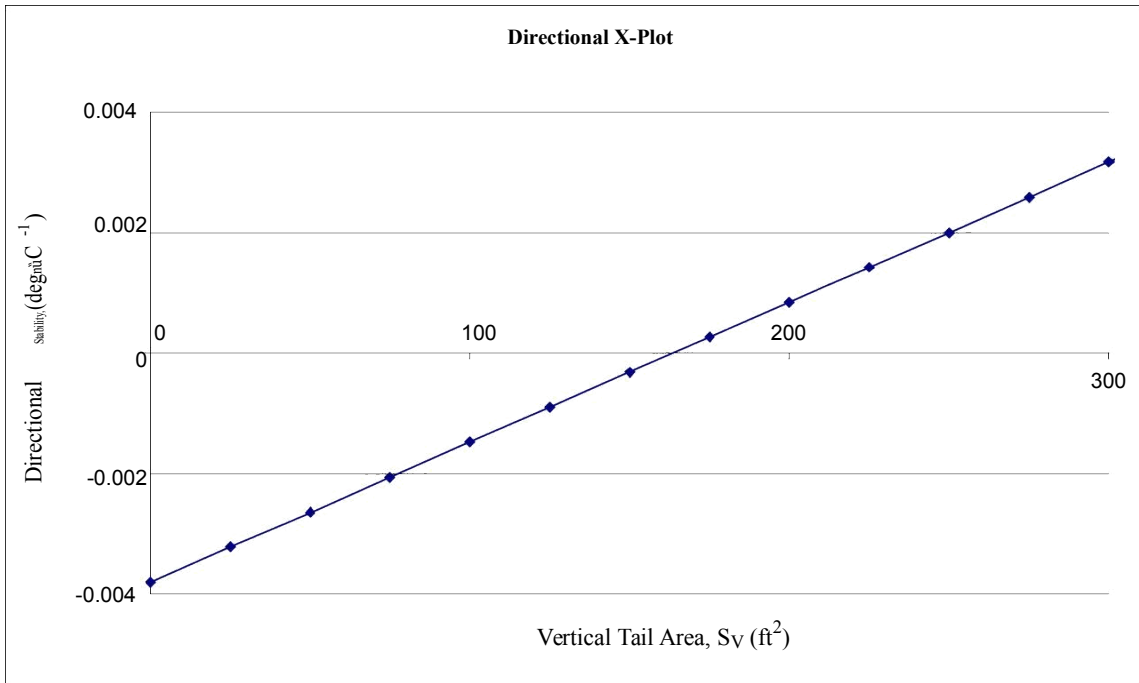
the weight analysis.

Figure 40. Directional X-plot

The $C_{n\beta}$ leg of the X-plot follows from:

$$C_{n_E} C_{n_E} \quad C_{L_D} (\frac{S_v}{V})(\frac{X_v}{V}) \tag{62}$$

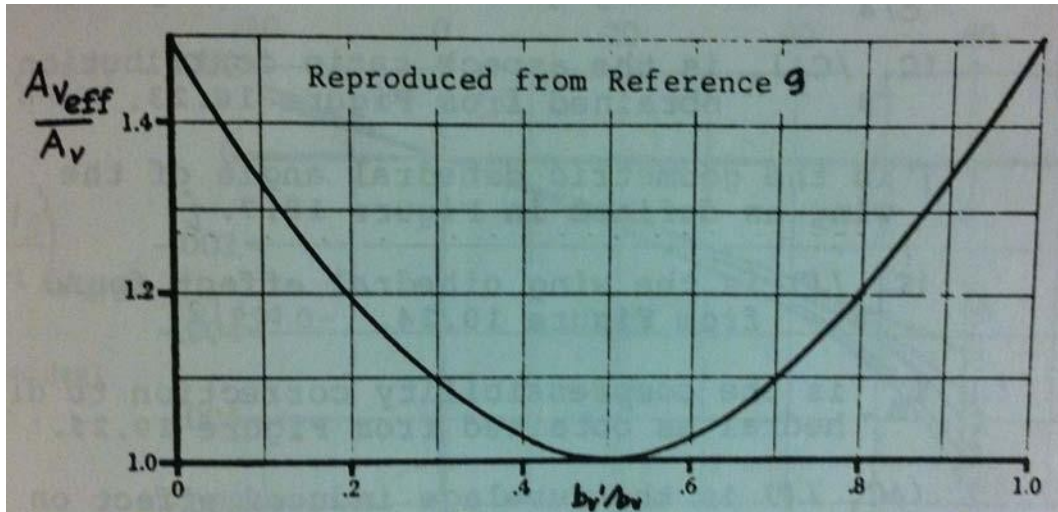For twin vertical tails, the effective aspect ratio of the vertical tail may be estimated from

figure 35:

Figure 41. Effective value of vertical tail aspect ratio

From empennage calculations, we have

b_v = 13 ft, S_v = 169 ft^2

by using these values we get,

A_v = 1.664

The vertical lift curve slope may be estimated from the following equation.

$$C_{L_{D_v}} \frac{2SA_{veff}}{[2 + \{\sqrt{\frac{A_{veff}^2 E^2}{k^2(\frac{1 + \tan^2 l_{c/2}}{E^2})} + 4\}]}$$

$$CL_{[v} = 2\Lambda A_{veff}/ [2 + \{A_{veff}^2 ü^2 /k^2 (1+ \tan^2 å_{c/2} /ü^2)$$

$+4\}^{1/2}$ (63)

By substituting the above calculated values in above equation, we get,

$CL_{[v}$ = 1.69 rad^{-1}

The fuselage contribution is calculated by,

$$C_{n_{E_f}} \quad \frac{57.3 K_N K_{R_l}}{(\frac{S_{fs} l_f}{Sb})}$$

(64)

Where:

K_N is empirical factor determined from Figure 42.

K_{Rl} a factor dependent on Reynold''s number and obtained from Figure 43.

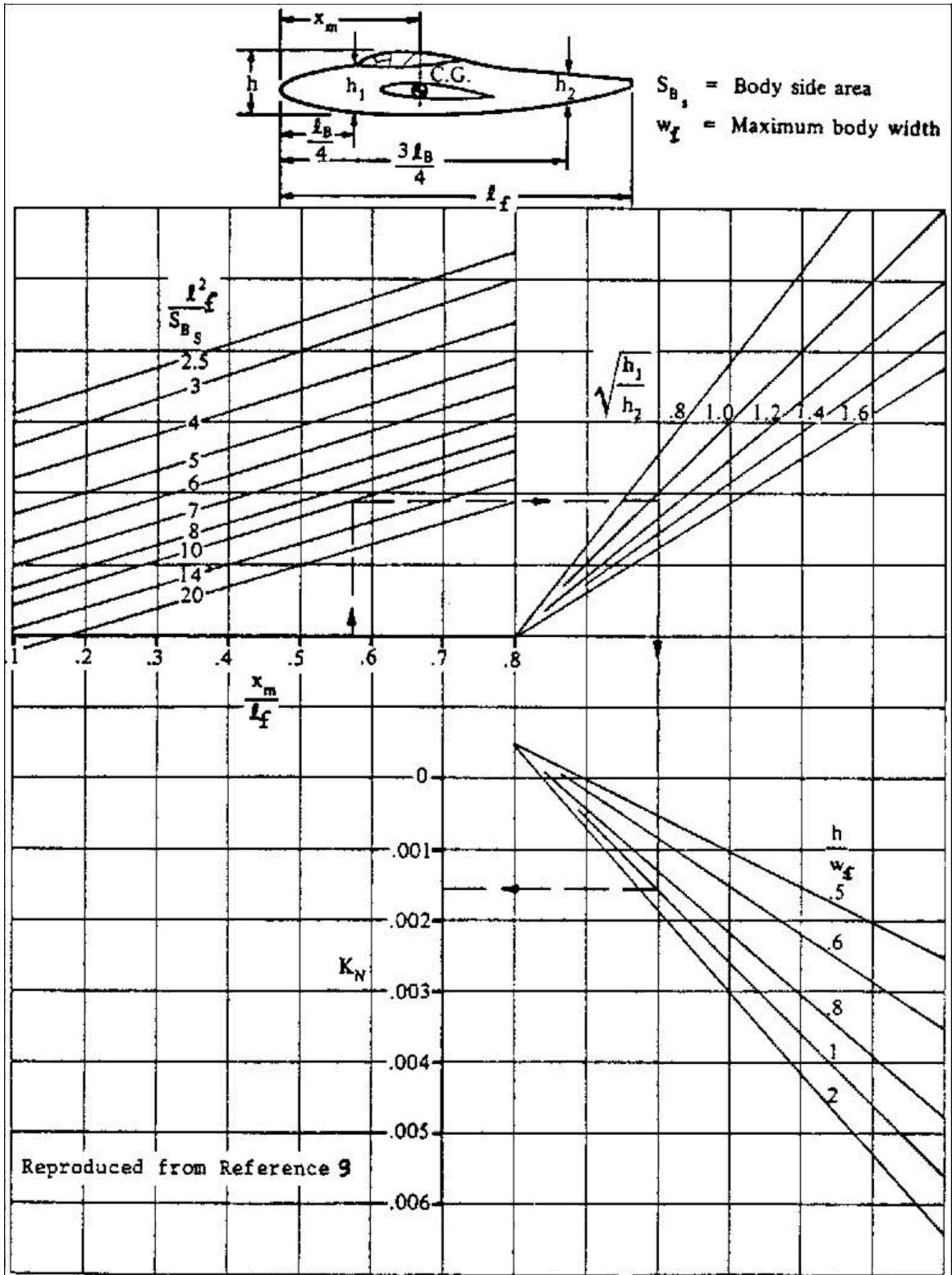S_{fs} and l_f are defined in Figure 43.

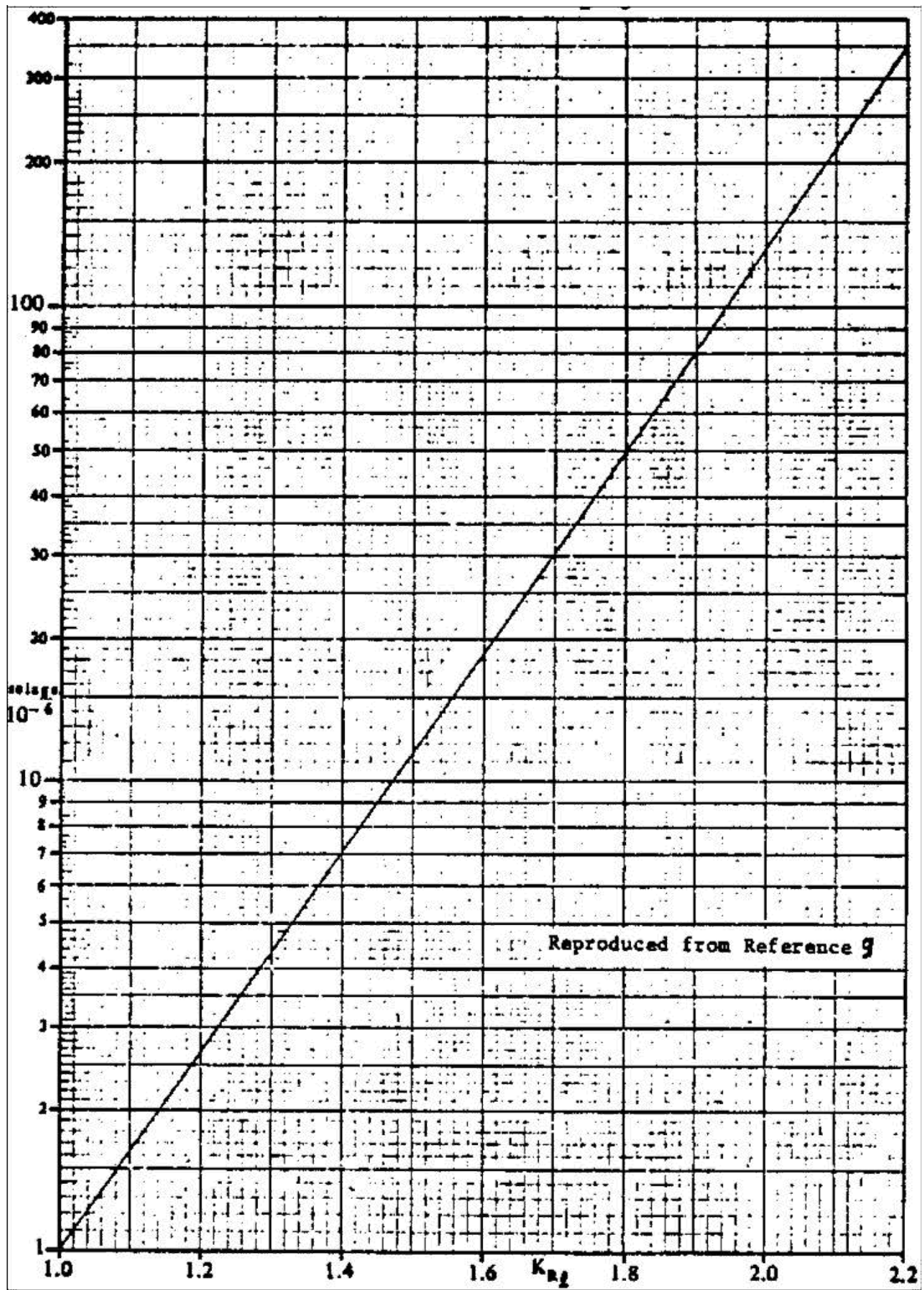Figure 42. Factor accounting for wing-fuselage interference with directional stability [11]

Figure 43. Effect of fuselage Reynolds number on wing fuselage directional stability [11]

By substituting these values in equation, we get

$C_{n\dot{u}}$ = -0.038

Chapter 10. Drag Polar

Before we determined the drag, one needs to calculate whether the Hoverwing will

sink or float when speed is 0. In order to calculate buoyancy force, one needs to

determine water displacement, which can be calculated by below equation. V = 35W

Buoyancy = d_e*V

d_e for salt water is 64 lb/ft^3. Buoyancy force works out to be 73,920 lbs, while

Hoverwing weighs 66,333 lbs. If Hoverwing weighed more than 73,920 lbs, it would

sink but since it does not weigh more than 66,333 lbs, it will float.

In order to calculate zero lift drag, it is important to calculate total wetted area of the

aircraft. The wetted area of the airplane is the integral of airplane perimeter versus

distance from nose to tail. A convenient way to find the wetted area is to split the airplane

into components such as,

1. Fuselage

2. Wing

3. Empennage

4. Nacelles

5. Other contributions which contribute to wetted area

Wetted areas for Planforms

The wetted area for the proposed design is calculated by,

$$ S_{wet\,plf} \quad 2S_{exp.\,plf} \quad \{1 \frac{0.25(t/c)_r\,(1\,WO)}{(1\,O)} \} \tag{65}$$

Where $IJ = (t/c)_r / (t/c)_t$ and $3 = c_t/c_r$

From all the parameters obtained in section 6 and 7 and by substituting the values in equation, we get

$S_{wetplf} = 1296$ ft^2

Wetted area for fuselage

The wetted area for fuselage is calculated by,

$$S_{wet_{fus}} \quad 3D_f l_f \; (1 \; \frac{2}{O_f})^{0.66} (1 \; \frac{1}{O_{f\,2}}) \tag{66}$$

Where $O_f \quad \dfrac{l_f}{D_f}$

From CAD drawings, we have,

$D_f = 43$ ft, $l_f = 73$ ft

By substituting the values in above equation, we get

$S_{wetfus} = 3,304$ ft^2

Wetted area for Nacelles

The following components of the nacelle contribute to wetted area: fan cowling, gas generator cowling and the plug. The wetted area for these components is calculated by,

$$S_{wet_{fancowl}} \quad l_{nn} D \{2 \quad \frac{l}{l_n} \quad \frac{0.8l_{si} D}{l_n D_n} \quad 1.15(1 \; \frac{l}{l_n})(\frac{D_{ef}}{D_n})^{0.35} \} \tag{67}$$

$$S_{wet_{gas\,gen}} \quad 3l_g D_g [1 \quad (\quad \frac{1}{3})(1 \quad \frac{D_{eg}}{D_g})\{1 \quad 0.18(\frac{D_g}{l_g})^{1.6} \}] \tag{68}$$

$$S_{wet_{plug}} \quad 0.73l_p D_p \tag{69}$$

By substituting the values in above equations, we get

$S_{wetfancowl.} = 285 \text{ ft}^2$

$S_{wetgas\ gen.} = -10 \text{ ft}^2$

$S_{wet\ plug} = 60 \text{ ft}^2$

<u>Wetted area for Horizontal tail</u>

The wetted area for horizontal tail is calculated by,

$$S_{wet_h} \quad 2S_h\ \{1 \quad \frac{0.25(\frac{t}{c}\big/)_r\ (1\ WO)}{(1\ O)}\ \} \tag{70}$$

From empennage calculations, we have

$S_h = 630 \text{ ft}^2 \qquad \quad \lambda_h = 0.57$

$S_v = 169 \text{ ft}^2 \qquad \quad \lambda_v = 0.58$

By substituting the values in above equation, we get

$S_{wet_h} \text{ ft}^2 = 350$

<u>Wetted area for Vertical tail</u>

The wetted area for vertical tail is calculated by,

$$S_{wet_v} \quad 2S_v\ \{1 \quad \frac{0.25(\frac{t}{c}\big/)_r\ (1\ WO)}{(1\ O)}\ \} \tag{71}$$

By substituting the values in above equation, we get

$S_{wetv} = 237 \text{ ft}^2$

Total wetted area $= S_{wetplf} + S_{wetfus} + S_{wetfancowl.} + S_{wetgas\ gen.} + S_{wet\ plug} + S_{weth} + S_{wetv}$ −−

intersection of wing and fuselage

$S_{wet} = 5,250$ ft^2

Comparing with reference [5], shows that for transport jets with a take off weight, of 66,333 lbs the wetted area is predicted to be 5,270 ft^2.

This is with in the 10% expected in the wetted area correlations.

x Equivalent Parasite drag of the airplane ''f''

The equivalent parasite drag of the proposed airplane is f = 21 ft^2.

x Clean Zero ––lift drag coefficient C_{Do}

The clean zero loft drag coefficient is calculated by,

$$C_{Do} \quad f\!\!\diagup\!\!S$$

By substituting the values, we get

$C_{Do} = 0.004$

The total craft drag before take-off can be expressed as follows:

$$D = D_{hw} + D_{hf} + D_{sww} + D_{swf} + D_{aw} + D_a + D_{fl} \tag{72}$$

After craft take-off, the total drag can be expressed as follows:

$$D = D_{aw} + D_a \tag{73}$$

The total drag and each separate drag component are discussed in the following.

The determination of craft drag is divided into four steps linked to the operating modes, i.e. boating; hovering or planing before take-off; at take-off while still on water surface; and in flying mode [12].

10.1. Wave-making drag

The Wave-making resistance is affected by beam to length ratio, displacement, shape of hull, Froude number. The wave-making resistance due to air cushion pressure under the main wings can be predicted based on Newman and Poole''s formula as follows:

$$D_{aw} = C_w B_c P_c^2 \tag{74}$$

$$C_w = f\ (F_{rc}, C/B_c) \tag{75}$$

$$F_{rc} = V/\mathrm{Sqrt}\ (gC) \tag{76}$$

For approximate calculation, this can be written as:

$$P_c = kW/\ (B_c Cn_{ac}) \tag{77}$$

Where

k Coefficient for estimating the proportion of the weight lifted by craft air cushion on water surface, 0.8.

C_w is calculated to be 0.0638 from above equation using weight of 66333 lbs, air cushion channel width of 21.9 ft, and Froude number of 1.76.

10.2. Drag due to the wetted surface on hull and side buoys

The drag caused hull and side buoys can be estimated as follows:

$$D_{hf} = (C_f + \mathrm{Delta}\ C_f)\ S_{hf} q \tag{78}$$

$$D_{swf} = (C_f + \mathrm{Delta}\ C_f)\ S_{swf} q \tag{79}$$

$$C_f = 0.075/\ (\log Re - 2)^2 \tag{80}$$

$$Re = l_s V_s / \hat{U}_w \tag{81}$$

For Reynolds number of 2.31×10^7, the skin friction drag is 0.0026.

Delta C_f is additional drag caused by roughness of the plate, which is estimated to be roughly 10-20% of C_f. C_{dhf} and C_{dswf} is calculated to be 0.0856 and 0.00546, accordingly.

10.3. Air profile drag

Air profile drag can be predicted based on model experiments in wind tunnel.

$$D_a = 1/2 \, d \, V^2 \, C_x S_a \tag{82}$$

In general, the air drag coefficient can be expressed as:

$$C_{d,a} = C_{xo} + K(h) C_L^2 / \Lambda A \tag{83}$$

For $C_L = 1.8$, $A = 3.45$, $C_{xo} = 0.002$ which is obtained from figure in reference [14],

and $K(h) = 0.2$ which is obtained from reference [14], C_a is 0.0612.

10.4. Fouling drag

Since the total drag of WIG Craft is rather small compared with conventional ships, the drag caused by the fouling is more significant, particularly during take-off, as it effects the drag and also the lift acting on both hull and sidewall/side buoys. However, in case of newly built craft or models, this drag component can be neglected. A factor does need to be added for performance reduction in service; however, as the hull surfaces will never be perfectly clean, a suggested factor is to increase the skin friction drag by 10%, which is 0.000061.

The equations for the boating, planing before take-off, at take-off while still on water surface and in flying mode of the proposed design are as follows:

Low speed, clean: $C_D = 0.004 + 0.03744 \, C_L^2$

Boating: $C_D = 0.077 + 0.03798 \, C_L^2$

Planing before take-off: $C_D = 0.102 + 0.03798 \, C_L^2$

At take-off while still on water surface: $C_D = 0.222 + 0.0424 \, C_L^2$
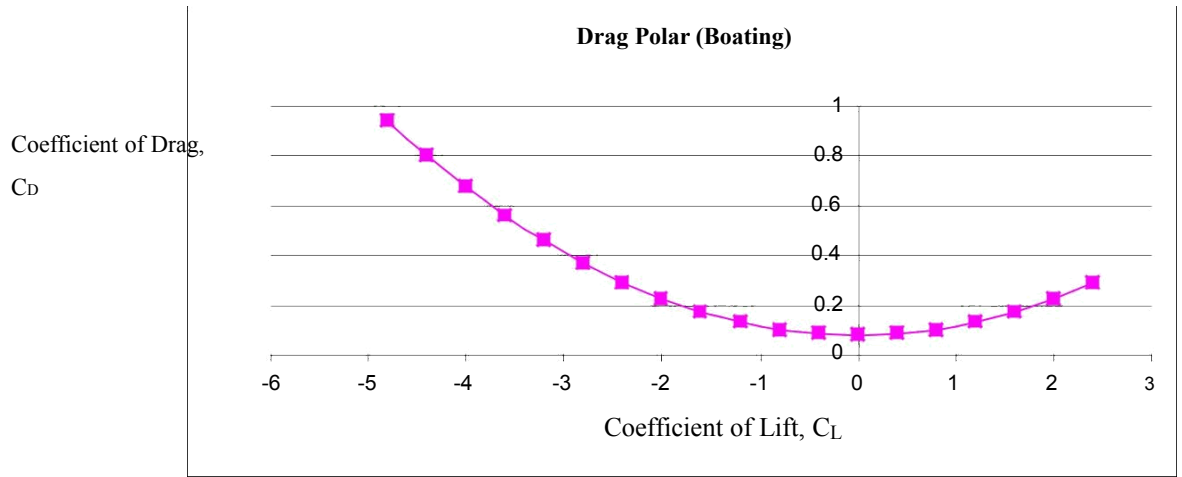
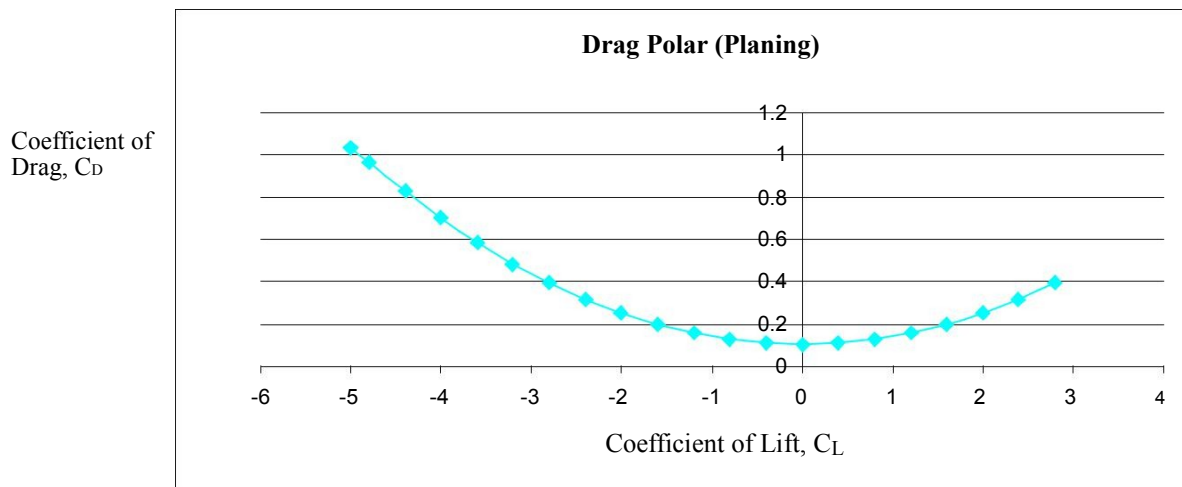Cruise: $C_D = 0.125 + 0.0424 \, C_L^2$

Drag Polar (Boating)

Coefficient of Drag, C_D

Coefficient of Lift, C_L

Figure 44. Drag Polar (Boating)

Drag Polar (Planing)

Coefficient of Drag, C_D

Coefficient of Lift, C_L

Figure 45. Drag Polar (Planing)

Drag Polar (At takeoff, while still on water)

Coefficient of Drag, C_D

Coefficient of Lift, C_L
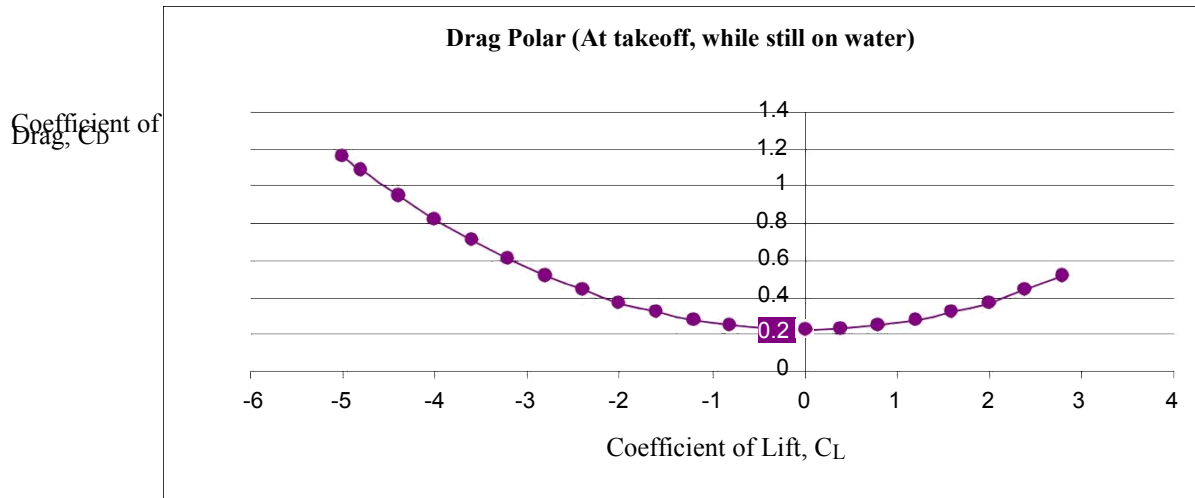
Figure 46 Drag Polar (At takeoff, while still on water)

Drag Polar (Cruise)

Coefficient of Drag, C_D
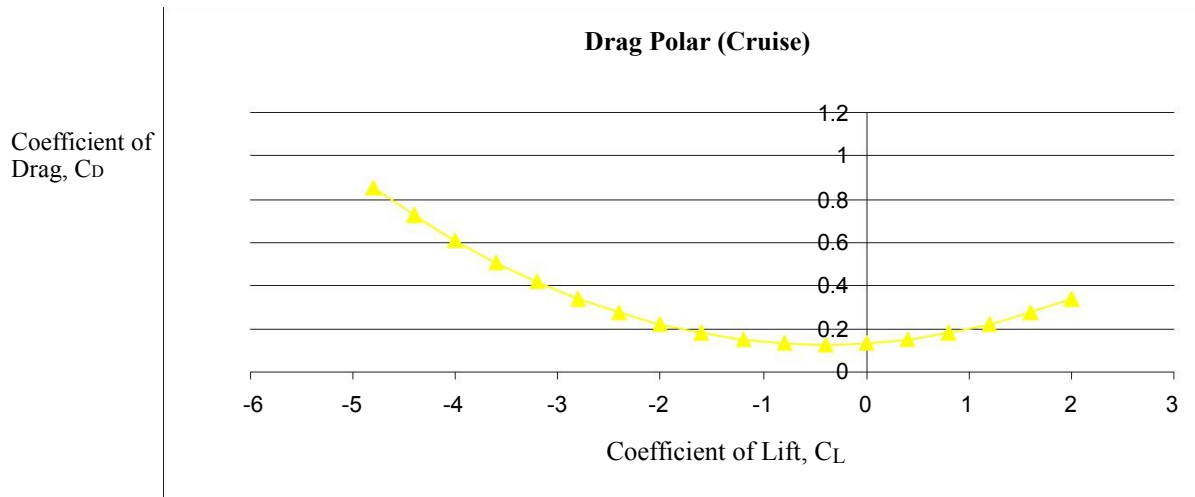
Coefficient of Lift, C_L
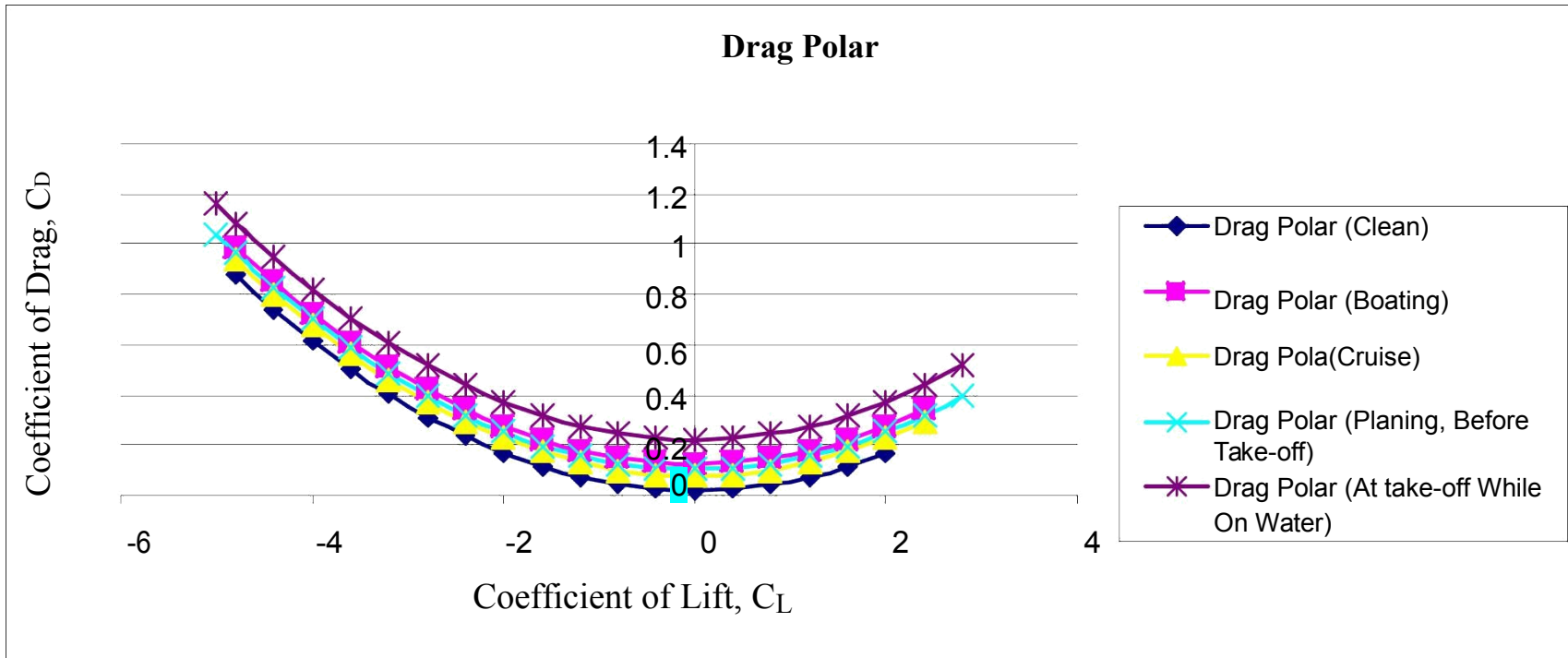
Figure 47. Drag Polar (Cruise)

Figure 48. Drag Polar

Chapter 11. V-n diagram

The V-n diagrams are used to determine design limit and design ultimate load factors as well as the corresponding speeds to which airplane structures are designed. Figure 85 shows the V-n diagram for the proposed design. The mission specification for the proposed aircraft is based on FAR 25 requirements. It will be assumed that under FAR 25 and will be certified under this category.

Determination of +1g stall speed: V_S

The design stall speed is given by,

$$V_S 2 \sqrt{\frac{(\frac{GW}{S})}{UC_{N_{max}}}} \qquad (84)$$

From weight sizing calculations, we have

GW = flight design gross weight in lbs = 66,333 lbs

S   = wing area in ft^2 = 3,175 ft^2

d = air density in slugs/ft^3 = 0.002378 slugs/ft^3

C_{Nmax} = maximum normal force coefficient

C_L = 1.4

In preliminary design it is acceptable to set:

C_{Nmax} = 1.1 C_{Lmax}

By substituting the values in above equation, we get

V_S = 105 kts

Determination of design cruising speed: V_C

The design cruise speed is given by,

$$V_C \ t \ V_B$$

43 Knots

Where

V_B = design spe

ed for maximum gust intensity We have $V_B = 163$ kts,

As $V_B \mathbf{t} V_A \mathbf{t} V_S \sqrt{n_{\lim}}$ (85)

By substituting the values in above equation, we get $V_c = 206$ kts   (86)

Determination of V_D:

The design dive speed is given by,

$V_D \quad 1.25 V_C$

By substituting the values in above equation, we get $V_D = 257$ kts   (87)

Determination of $n_{\lim}$:

The positive limit load factor for the proposed design is given by,

$$n_{\lim\ pos} \mathbf{t} 2.1 \quad \{ \frac{24{,}000}{(GW\ 10000)} \}$$

By substituting the values in above equation, we get $n_{\lim pos} = 2.41$ (88)

Determination of gust load factor lines, V_C, V_B and V_D:

The airplane mass ratio is given by,

$$P_g \quad 2\frac{(GW / S)}{\overline{U}cgC_{LD}}$$

     (89)

By substituting the values in above equation, we

get $3_g = 17$

The gust alleviation factor is given by,

$$K_g \quad \frac{0.88 P_g}{(5.3 \ P_g)} \tag{90}$$

By substituting the values in above equation, we

get $K_g = 0.67$

The gust load factor is given by,

$$n_{lim} \quad 1 \quad \frac{(K_g U_{de} V C_{LD})}{498 \left(\frac{GW}{S} \right)} \tag{91}$$

For the V_C gust lines, $U_{de} = 50$ fps

For the V_D gust lines, $U_{de} = 25$ fps

For the V_B gust lines, $U_{de} = 66$ fps

By substituting the values in above equation, we

get $n_{limgust} = 1 + 3.22 * 10^{-3} V$ for the V_C line.

$n_{limgust} = 1 + 1.61 * 10^{-3} V$ for the V_D line.

$n_{limgust} = 1 + 4.25 * 10^{-3} V$ for the V_B line.

Determination of V_A:

$$V_A \quad t \sqrt{V_S} n_{lim} \tag{92}$$

By substituting the values in above equation, we

get $V_A = 146$ kts

Determination of negative stall line: V_{Sneg}

It is assumed that $C_{Lmaxneg} = -1.0$. This yields $C_{Nmaxneg} = -1.1$

The negative stall speed is calculated by,

$$V_{Sneg} = \sqrt{\frac{(GW/S)}{UC_{N_{max\,neg}}}}$$

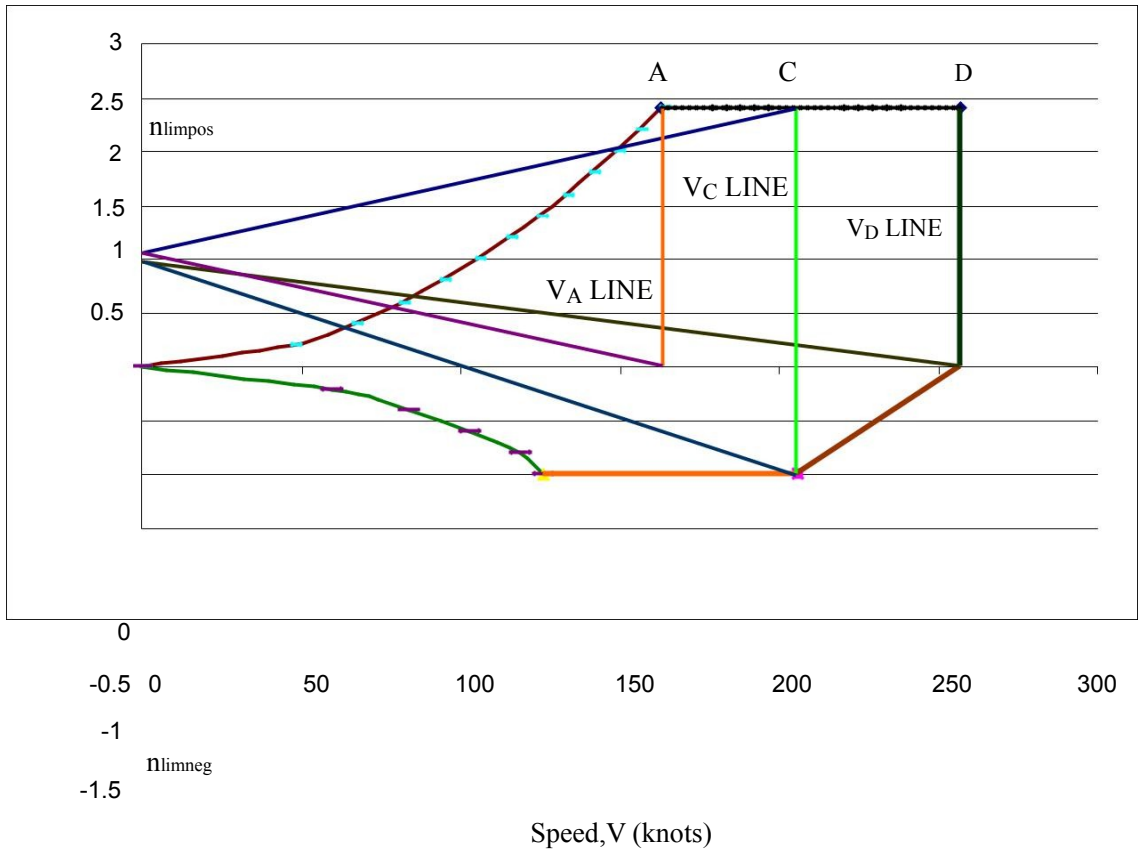By substituting the values in above equation, we get

$V_{Sneg} = 126$ kts.

Figure 49. V-n Diagram

Chapter 12. Conclusion

The Hoverwing is a unique craft which is a mix between a ship and an airplane. As seen from above data, the manual calculations of all the parameters are more reliable than those obtained from AAA software. The airplanes with takeoff values closest to Hoverwing were taken into consideration when calculation drag, horizontal and vertical stabilizer. Though this method would not give a larger error margin, it is better than computing in AAA software as the software compares and uses the values for airplanes that are into certain categories such as military, jet transport, flying boat, etc. To obtain the data, flying boats were used as a comparison. When the data for flying boats was not available, the aircraft with similar takeoff weight was taken into consideration. The category with similar takeoff weight was commercial transport aircraft. The weight sensitivity results were obtained within 0.5% error margin. The CAD drawing of Hoverwing is shown in figure 50.
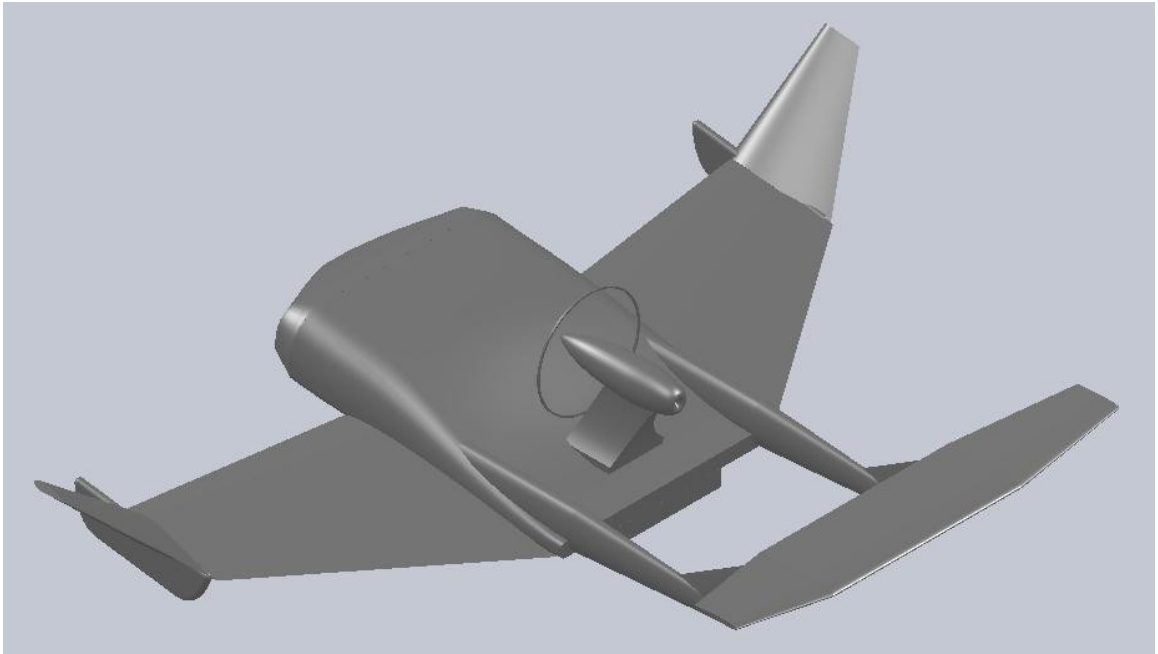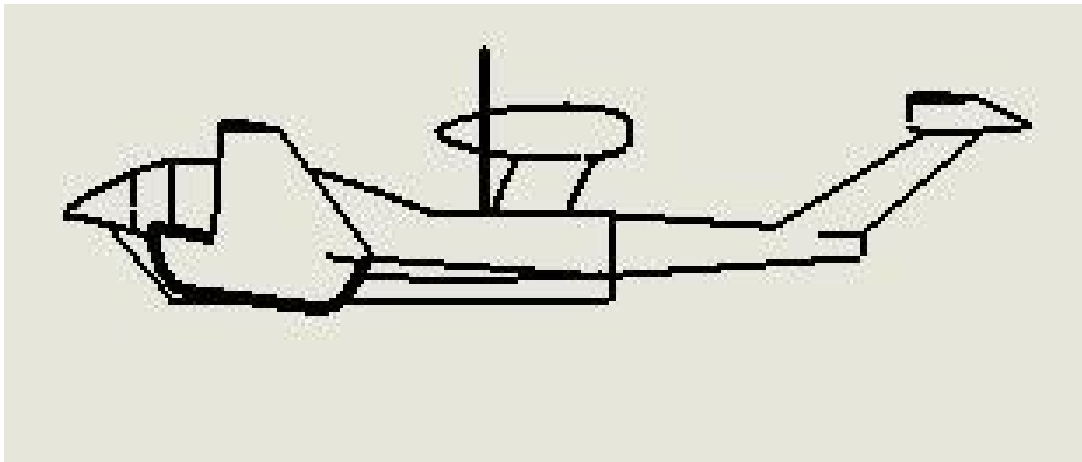
Figure 50. 3D view of hoverwing
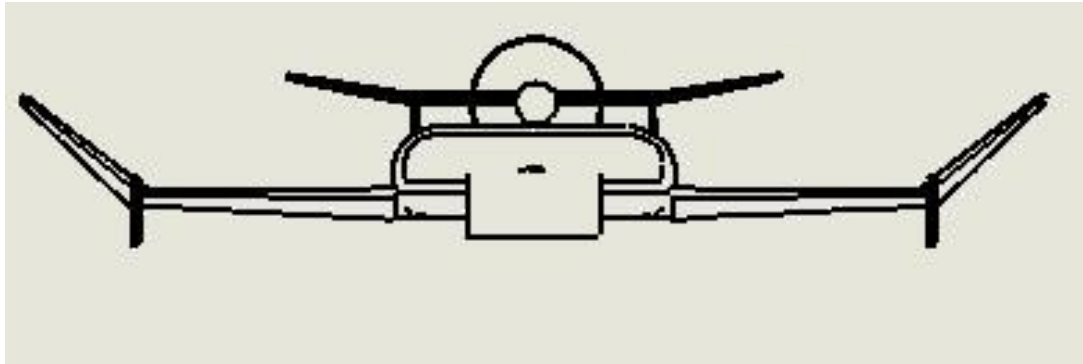

Figure 51. Side view of hoverwing
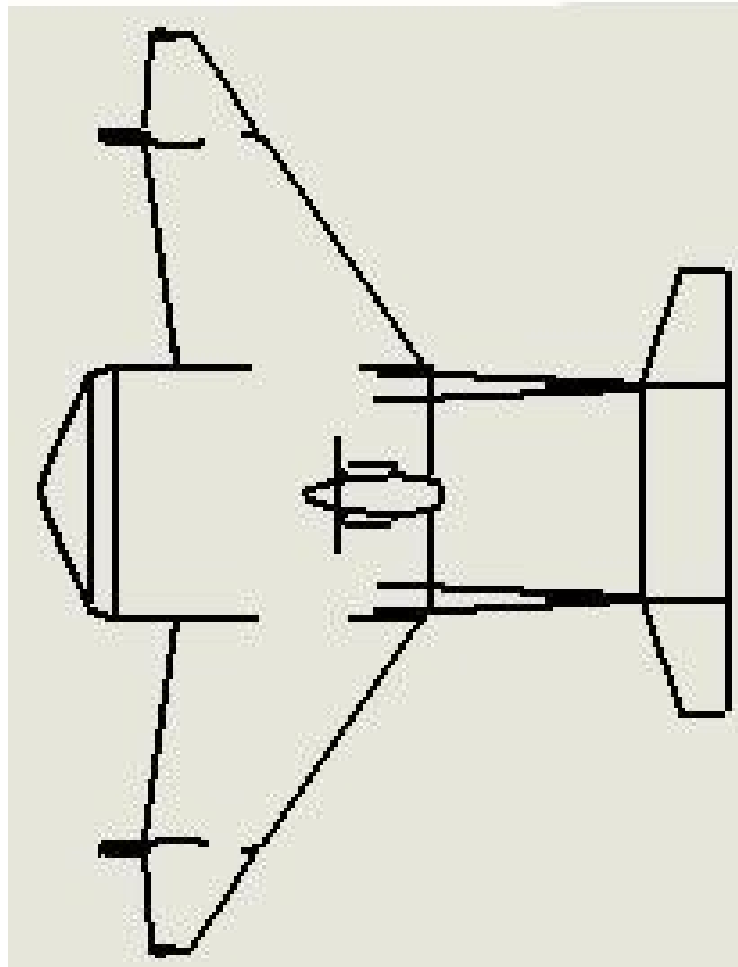
Figure 52. Front view of hoverwing

Figure 53. Top view of hoverwing

The drag calculation has been completed for the Hoverwing. As seen from the drag polar,

the highest drag was encountered when Hoverwing is transiting from air to water. This

data is correct since WIG crafts require more power to overcome hump speed drag.

Hoverwing will not have any landing gear as it takes off, lands and operates on water. As seen from weight and balance analysis, Hoverwing is capable of flying in all 5 scenarios with C.G. movement. Overall, if this design was used to produce a real craft, it would be successful.

Hoverwing is about series/mass production of high speed marine craft at a manufacturing scale similar to the volume of the speedboat sector. The market potential for Hoverwing is enormous. In the end, Hoverwing is simply about being a fast, comfortable transportation solution which requires little other infrastructure investment. Making Hoverwing commercially successful is a long journey, but it is a venture worth exploring.

Chapter 13. References

[1] Taylor, G. *WIG –– What Are You Waiting For?* International Conference on Fast Sea Transportation FAST''2005, St.Petersburg, Russia, 2005.

[2] Rozhdestvensky, K. *Wing-in-ground effect vehicles*. 9th International Conference on Hydrodynamics, Shanghai, China, 2010.

[3] Fischer, H., and Matjasic, K. *The Hoverwing Technology-Bridge between WIG and ACV*. RTO MP-15, Amsterdam, the Netherlands, 1998.

[4] Taylor, G. *The 90 Knot Zero-Wash Ferry*. The Pacific 2004 International Maritime Conference, Sydney, Australia, 2004.

[5] Roskam, Dr. Jan. *Part I: Preliminary Sizing of Airplanes*. DAR Corporation, Kansas, 2004.

[6] Marchman, J., and Werme, T. *Clark-Y Airfoil Performance at Low Reynolds Numbers*. AIAA 22nd Aerospace Sciences Meeting, Reno, Nevada, 1984.

[7]   Roskam, Dr. Jan. *Part III: Layout Design of Cockpit, Fuselage, Wing and Empennage: Cutaways and Inboard Profiles*. DAR Corporation, Kansas, 2004.

[8] Torenbeek, E. *Synthesis of Subsonic Airplane Design*. Kluwer Academic Publishers, Dordrecht, the Netherlands, 1982.

[9] Roskam, Dr. Jan. *Part V: Component Weight Estimation*. DAR Corporation, Kansas, 2004.

[10]   Halloran, M. and O''Meara, S. *Wing in Ground Effect Craft Review*. DSTO Aeronautical and Maritime Research Laboratory, Melbourne, Australia, 1999.

[11]   Roskam, Dr. Jan. *Part VI: Preliminary Calculation of Aerodynamic, Thrust and*

Power Characteristics. Airplane Design. Kansas, 2004.

[12] Yun, L., Bliault, A., and Doo, J. *WIG Craft and Ekranoplan: Ground Effect Craft Technology*. Springer New York Dordrecht Heibelderg, London, 2009.